construction engineering research laboratory

TECHNICAL REPORT N-38
February 1978

Prediction of the Noise Impact Within and Adjacent to Army Facilities

ROTARY-WING AIRCRAFT OPERATIONAL NOISE DATA

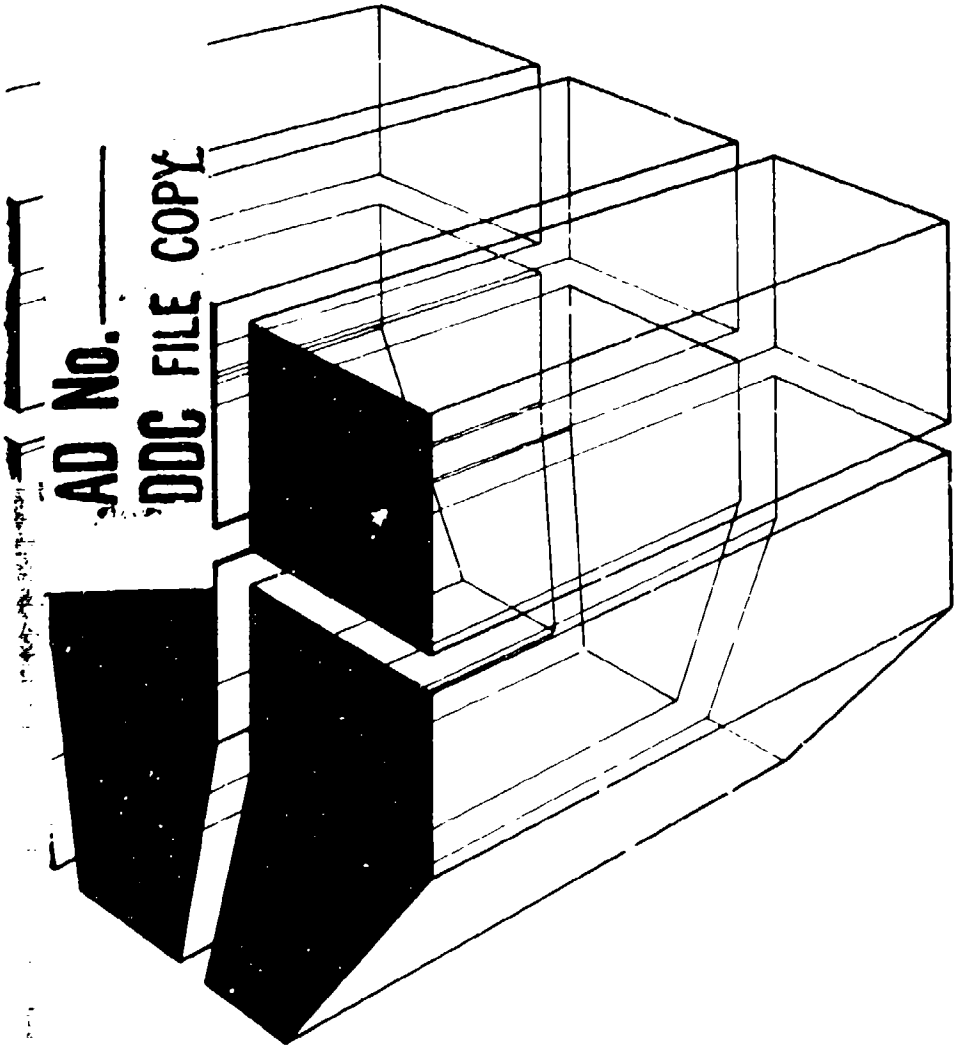

by
B. Homans
L. Little
P. Schomer

CERL

The contents of this report are not to be used for advertising, publication, or promotional purposes. Citation of trade names does not constitute an official indorsement or approval of the use of such commercial products. The findings of this report are not to be construed as an official Department of the Army position, unless so designated by other authorized documents.

DESTROY THIS REPORT WHEN IT IS NO LONGER NEEDED
DO NOT RETURN IT TO THE ORIGINATOR

DISCLAIMER NOTICE

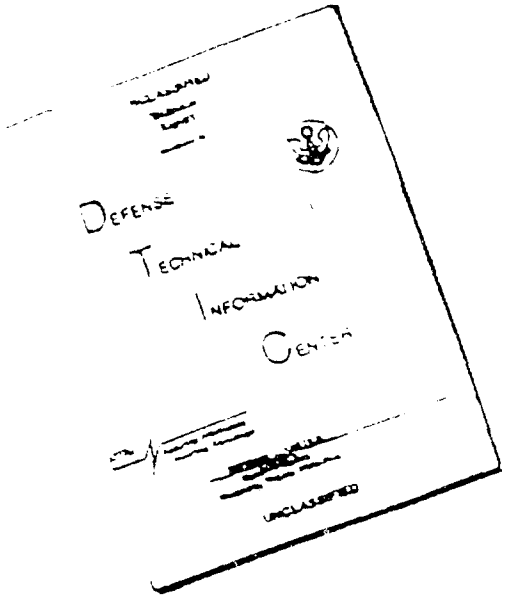

THIS DOCUMENT IS BEST QUALITY AVAILABLE. THE COPY FURNISHED TO DTIC CONTAINED A SIGNIFICANT NUMBER OF PAGES WHICH DO NOT REPRODUCE LEGIBLY.

SECURITY CLASSIFICATION OF THIS PAGE (When Data Entered)

REPORT DOCUMENTATION PAGE

READ INSTRUCTIONS BEFORE COMPLETING FORM

1. REPORT NUMBER: CERL-TR-N-38	2. GOVT ACCESSION NO.
3. RECIPIENT'S CATALOG NUMBER	
4. TITLE (and Subtitle): ROTARY-WING AIRCRAFT OPERATIONAL NOISE DATA.	5. TYPE OF REPORT & PERIOD COVERED: FINAL rept.
6. PERFORMING ORG. REPORT NUMBER	
7. AUTHOR(s): B. Homans, L. Little, P. Schomer — Brian Homans, Lincoln Little, Paul D. Schomer	8. CONTRACT OR GRANT NUMBER(s)
9. PERFORMING ORGANIZATION NAME AND ADDRESS: CONSTRUCTION ENGINEERING RESEARCH LABORATORY, P.O. Box 4005, Champaign, Illinois 61820	10. PROGRAM ELEMENT, PROJECT, TASK AREA & WORK UNIT NUMBERS: 4A762720A896-03-001
11. CONTROLLING OFFICE NAME AND ADDRESS	12. REPORT DATE: Feb[illegible] 1978
	13. NUMBER OF PAGES: 69
14. MONITORING AGENCY NAME & ADDRESS (if different from Controlling Office): 77p.	15. SECURITY CLASS. (of this report): Unclassified
	15a. DECLASSIFICATION/DOWNGRADING SCHEDULE

16. DISTRIBUTION STATEMENT (of this Report)

Approved for public release; distribution unlimited.

DDC RECEIVED APR 3 1978 F

17. DISTRIBUTION STATEMENT (of the abstract entered in Block 20, if different from Report)

18. SUPPLEMENTARY NOTES

19. KEY WORDS (Continue on reverse side if necessary and identify by block number)

rotary-wing aircraft
dynamic operations
noise impact

20. ABSTRACT (Continue on reverse side if necessary and identify by block number)

This report presents Sound Exposure Level (SEL) vs distance curves for eight models of Army rotary-wing aircraft (OH-58, AH-1G, UH-1M, UH-1H, UH-1B, CH-47B, CH-54, and TH-55) performing dynamic operations, and Equivalent Sound Level (L_{eq}) contours for the same aircraft in static operations. The dynamic operations consisted of level fly-overs, ascents, descents, turns, takeoffs, and landings; static operations included in-ground and out-of-ground effect hovers. Results are grouped according to model and type of operation and are suitable for use in manual or computerized programs for predicting noise impact from rotary-wing aircraft.

DD FORM 1 JAN 73 1473 EDITION OF 1 NOV 65 IS OBSOLETE

UNCLASSIFIED SECURITY CLASSIFICATION OF THIS PAGE (When Data Entered)

FOREWORD

This research was conducted for the Directorate of Military Construction, Office of the Chief of Engineers (OCE) under Project 4A762720A896, "Environmental Quality for Construction and Operation of Military Facilities"; Task 03, "Noise Pollution Control for Military Facilities"; Work Unit 001, "Prediction of the Noise Impact Within and Adjacent to Army Facilities." The applicable QCR is 1.03.011. Mr. Frank P. Beck, DAEN-MCE-P, was the OCE Technical Monitor.

The work was performed by the Acoustics Team (ENA) of the Environmental Division (EN), U.S. Army Construction Engineering Research Laboratory (CERL). Dr. P. Schomer is Chief of ENA and Dr. R. K. Jain is Chief of EN.

COL J. E. Hays is Commander and Director of CERL and Dr. L. R. Shaffer is Technical Director.

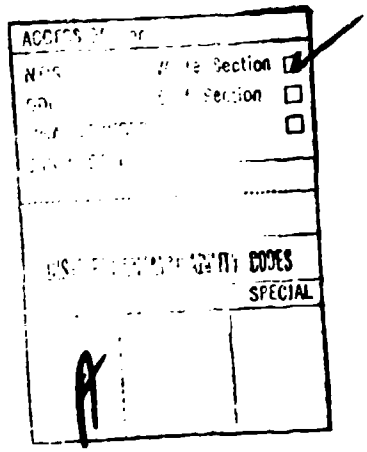

CONTENTS

TABLES

FIGURES

FIGURES (cont'd)

ROTARY-WING AIRCRAFT OPERATIONAL NOISE DATA

1 INTRODUCTION

Background

U.S. Army Construction Engineering Research Laboratory (CERL) research into the prediction and assessment of the noise impact on and adjacent to Army facilities has identified blast noise, rotary-wing aircraft, vehicles, and fixed sources as major noise sources, with blasts and rotary-wing aircraft selected as the major problems.

Urban development has been encroaching on military and civilian airfields in recent years. In particular, residential development has been occurring in areas subject to high noise levels emanating from aircraft and airfield operations.

The *Construction Criteria Manual*[1] and the *Air Installations Compatible Use Zones*[2] are two Department of Defense (DOD) documents that define land-use restrictions. Both documents describe three zones which impose varying degrees of restriction on land use in order to insure its compatibility with the characteristics of Army operations. Meeting these restrictions, however, requires that the noise impact of Army operations be predicted.

Various manual and computerized procedures for predicting noise impact from fixed-wing aircraft have existed for about 10 years. The Air Force, in particular, has taken interest in this area because of its large fleet of jet aircraft. Because fixed-wing aircraft have somewhat limited maneuverability, a straightforward methodology, such as that of the Air Force,[3] can be used in predicting their noise impact. The Air Force procedure uses distinct flight paths and other operational information to predict noise impact. Unlike fixed-wing aircraft, however, helicopters are able to make tight turns and execute sharp maneuvers. Training procedures demand that helicopter pilots be proficient in this flexible form of flight. Because of the resulting impossibility of defining helicopter flight paths with current records, a straightforward procedure like the Air Force's does not work for rotary-wing aircraft.

CERL therefore developed guidelines for laying out corridors rather than defining distinct flight paths. These guidelines, presented in CERL Interim Report N-10,[4] enable the planner to establish state-of-the-art prediction capabilities and to provide a basis for more detailed analysis when actual aircraft operations are sufficiently well-documented to justify more precise procedures.

Purpose

The purpose of this study was to develop state-of-the-art Sound Exposure Level (SEL) vs distance curves in a form which will permit their use in manual or computerized prediction procedures.

Approach

A number of preliminary steps were required before rotary-wing SEL vs distance tables could be generated. First, noise from a UH-1 aircraft was measured at CERL in the spring of 1973 to ascertain expected noise levels in preparation for a full-scale measurement program of the Army's inventory of helicopters. The aircraft was flown at several altitudes until optimum recording levels could be found. During this period, several operations, such as level flight, ascents, descents, and turns, were experimented with, as was placement of microphones to form an array.

Following the initial measurements, a Joint Services Noise Exposure Forecast Technical Conference was held at CERL in October 1973 to develop the framework for a rotary-wing aircraft measurement plan. At this meeting, the inventory for measurement was decided upon, tracking methods were discussed, operations were ascertained, the altitudes at which the aircraft should fly were debated, conditions of loading were commented upon, a microphone array was layed out, instrumentation was outlined, and the method of initial analysis was enunciated briefly.

[1] *Construction Criteria Manual*, DOD 4270.1-M (Department of Defense, 1972).

[2] *Air Installations Compatible Use Zones*, DOD Instruction 4165-57 (Department of Defense, 1973).

[3] R. D. Horonjeff, et al., *Community Noise Exposure Resulting from Aircraft Operations: Computer Program Description*, Report AD/A-004821 (Bolt, Beranek and Newman [BBN], 1974).

[4] P. D. Schomer and B. L. Homans, *User Manual: Interim Procedure for Planning Rotary-Wing Aircraft Traffic Patterns and Siting Noise-Sensitive Land Uses*, Interim Report N-10/ADA031450 (U.S. Army Construction Engineering Research Laboratory [CERL], 1976).

Following this Joint Services conference, rotary-wing aircraft measurements were performed at Louisville stagefield near Fort Rucker, AL, in April 1974. The Fort Rucker locale was chosen because of the availability of rotary-wing aircraft. Louisville stagefield is outfitted for these measurements, is proximate to Fort Rucker, and was not used at the time for training purposes.

Louisville stagefield is comprised of four 1000-ft (305-m) hard-surfaced landing lanes and a large parking area. For dynamic operation measurements, Landing Lane 3 was instrumented with an array of six microphones and was overflown by aircraft executing 14 specific operations. Multi-track magnetic recordings were made of each operation. Static operation measurements and recordings were made on the parking area using a moving microphone. Chapter 2 details the helicopter operations and methods of measurement.*

Noise from eight types of Army helicopters was measured during these tests (Table 1). Lighter aircraft (such as OH-58, AH-1G, UH-1M, and TH-55) were tested with normal loading, while the utility and cargo types (UH-1H, UH-1B, CH-47, and CH-54) were measured normally and fully loaded because it was felt that the gross weight would affect performance, resulting in a change in sound pressure level. Auxiliary fuel tanks in the UH-1H and UH-1B aircraft were filled with gasoline to simulate full troop capacity; the CH-47 and CH-54 aircraft flew with external sling loads. A sampling of aircraft and pilots was requested from Fort Rucker to obtain model-to-model and pilot-to-pilot variability. When nonavailability of aircraft prevented this, a mix of pilots was obtained.

Following these measurements, data were reduced from the magnetic tape recordings (Chapter 3) and analyzed according to the Air Force Method[5] to generate preliminary SEL vs distance curves (Chapter 4). These data were qualified with meteorological measurements conducted during the study and combined to reflect SEL vs distance curves for various meteorological and operating conditions (Chapter 5).

*During the tests, a jury of 30 subjects judged helicopter noise compared to that of a fixed-wing (C-3) aircraft. Results of that companion study will be reported in a forthcoming CERL report entitled *Subjective Ratings of Annoyance Produced by Rotary-Wing Aircraft Noise.*

[5]D. E. Bishop and W. J. Galloway, *Community Noise Exposure Resulting from Aircraft Operations: Acquisition and Analysis of Aircraft Noise and Performance Data*, Report AMRL-TR-73-107 (BBN, 1975).

Table 1
Helicopter Types and Loading Conditions Measured at Fort Rucker, AL

Helicopter Model	Loading Condition
OH-58	Normal
AH-1G	Normal
UH-1M	Normal
UH-1H	Maximum or Normal
UH-1B	Maximum or Normal
CH-47B	Maximum or Normal
CH-54	Maximum or Normal
TH-55	Normal

Mode of Technology Transfer

This report is a basic document to support the *User Manual: Interim Procedures for Planning Rotary-Wing Aircraft Traffic Patterns and Siting Noise-Sensitive Land Uses*[6] and a planned computerized helicopter noise prediction contouring system.

2 COLLECTION OF DATA

Helicopter Operations

The purpose of the rotary-wing aircraft measurements conducted at Fort Rucker was to obtain baseline information for the creation of a prediction methodology by measuring portions of aircraft flight for all types of rotary-wing aircraft in the Army's inventory. To accomplish this, a series of operations was conceived that approximated portions of actual flight. In all, 14 dynamic operations were performed over a six-microphone stationary array, and two static (hover) operations were measured with a moving microphone. Analog tape recordings were made of the aircraft dynamic operations while cameras fixed the position of the aircraft in space.

The dynamic operations consisted of two level flyovers, two NOE* maneuvers, two ascents, two descents, two left turns, two right turns, one landing, and one

[6]P. D. Schomer and B. L. Homans, *User Manual: Interim Procedures for Planning Rotary-Wing Aircraft Traffic Patterns and Siting Noise-Sensitive Land Uses*, Interim Report N-10/ADA031450 (CERL, 1976).

*NOE (nap of the earth) operations were not reduced in final analysis due to the inability to predict aircraft flight.

takeoff. Static operations consisted of one in-ground and one out-of-ground effect hover. The 16 dynamic and static operations comprised a set.

Before and after each dynamic operation, pilots were instructed to maintain straight, level, steady flight for at least 1.5 n mi (2.8 km). All teardrop turns and other ancillary maneuvers in preparation for the actual dynamic operation were performed beyond the 1.5 n mi (2.8 km). In addition to allowing the pilot to stabilize the aircraft, the 1.5 n mi (2.8 km) gave sufficient time for 10-dB down points to be recorded on magnetic tape. Table 2 presents the dynamic operations and ground tracks from which operations were initiated.

The first level flyover was at an altitude of 300 ft (91 m), directly over Landing Lane 3 on a ground track of 360 degrees (Figure 1). After executing a teardrop turn, the aircraft again executed a level flyover at an altitude of 300 ft (91 m), but on a ground track of 180 degrees.

After executing a teardrop turn, the first ascent was initiated (Figure 2). Beginning at an altitude of 280 ft (85 m) AGL along a ground track of 360 degrees, straight, level flight was maintained until the aircraft was directly above the south edge of the runway. At this point, the aircraft began climbing at 500 ft/min (152 m/min) for 40 sec. After completion of the ascent (at about 600 ft [183 m]), the aircraft continued on a ground track of 360 degrees for 1.5 n mi (2.8 km).

The first descent was performed similarly (Figure 3). Straight, level flight was maintained at 320 ft (98 m) AGL on a ground track of 180 degrees. At the north edge of the runway, a descent of 500 ft/min (152 m/min) was made until 80 ft (24 m) AGL was reached. At that time, an ascent was made for 1.5 n mi (2.8 km). The second descent was flown on a ground track of 360 degrees and ascent was flown on a ground track of 180 degrees.

The first turn (Figure 4) was initiated at a point 1.5 n mi (2.8 km) southeast of the field. With a heading of 315 degrees at 300 ft (91 m) AGL, the helicopter approached the field at straight, level flight for at least 1 n mi (1.9 km). Upon reaching the field, a 90-degree turn to the port side was initiated. Turns were conducted at 3 degrees/sec and were intended to overfly the center of the landing lane when the aircraft was 45 degrees into the turn. When a heading of 225 degrees was reached, straight, level flight was maintained for 1 n mi (1.9 km).

Table 2
Dynamic Operations Performed at Fort Rucker

Operation	Beginning Ground Track (Degrees)
1. Level	360
2. Level	180
3. NOE*	360
4. NOE	180
5. Ascent	360
6. Descent	180
7. Descent	360
8. Ascent	180
9. Left turn	315
10. Right turn	45
11. Right turn	225
12. Left turn	135
13. Landing	180
14. Takeoff	180

*NOE operations were not used in the analyses because of the inability to predict aircraft position.

The second turn was initiated from a heading of 45 degrees at 300 ft (91 m) AGL. At the field, a 90-degree turn starboard at 3 degrees/sec was initiated until a heading of 135 degrees was reached. The third turn was started with a heading of 225 degrees. A 90-degree turn was initiated at the field until a heading of 315 degrees was reached. The fourth turn was started with a heading of 135 degrees. A 90-degree turn to the port side was initiated at the field until a heading of 45 degrees was reached.

The next maneuver, a normal landing (Figure 5), was initiated at 300 ft (91 m) AGL on a ground track of 180 degrees. Landing was accomplished 800 ft (244 m) south of the north edge of the landing lane. The aircraft then taxied to a point 200 ft (61 m) south of the north edge of the landing lane. Takeoff was accomplished on 180 degrees ground track.

Static operations consisted of in-ground and out-of-ground effect hovers. These measurements were performed over a hard-surfaced area (Figure 6). In-ground effect hovers were performed with the aircraft at a stabilized position between 0 and 5 ft (0 and 1.5 m) above the ground. The aircraft maintained the stabilized position by always facing into the wind. Out-of-ground hovers were performed at an altitude of one rotor diameter.

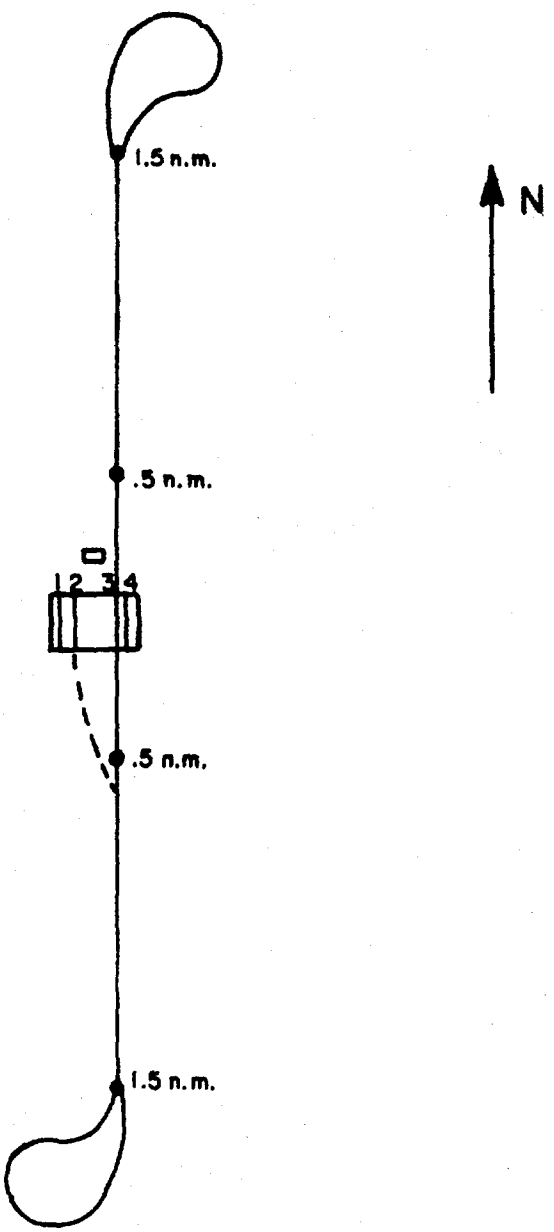

Figure 1. Flight path for level flyovers, ascents and decents.

Microphone Placement

An array of six microphones was chosen for the dynamic operation measurements (Figure 7). It was felt that the symmetrical arrangement of these microphones about the longitudinal axis of the landing lane would allow optimum recordings of takeoffs, landings, ascents, descents, and level flyovers (most flown in two directions), as well as turns. Microphone tripods adjacent to the hover area were cemented in concrete blocks to prevent their being blown over by high, aircraft-generated winds.

One boom-mounted microphone was used for static operation measurements. Measurements were made at intervals of 30 degrees around each aircraft at a 200-ft (61-m) radius (300 ft [91 m] for the CH-47 and CH-54 aircraft), while it performed an in-ground or out-of-ground effect hover. Measurement positions were marked with stakes so that they could be replicated for each aircraft.

Measurement Instrumentation

Acoustic instrumentation for the dynamic operation measurements (Figure 8a) consisted of six B&K 4149 1/2-in. (12.7-mm) quartz-coated microphones protected by B&K UA-0237 polyurethane windscreens and mounted on 4.5-ft (1.4-m) tripods. The microphone signal was fed into B&K 141 field preamplifiers which were in turn wired to the equipment van. In the van, each microphone signal was amplified by a Neff type 119 DC amplifier. Each amplified microphone signal was then split: one half of the signal was fed to one channel of the Ampex FR 1300 14-track tape recorder; the other half went through a 707-Hz high-pass filter, was amplified by another Neff amplifier, and was fed to one channel on the tape recorder. Thus, one channel of the tape recorder was fed directly, while the other was high-pass filtered.

The 707-Hz high-pass filter allowed for a greater dynamic range in recording without overloading from the low-frequency impulsive nature of the helicopter signature. To monitor overloads, each tape recorder channel was equipped with a latching level-comparator circuit. This circuit flagged suspect channels so that adjustments in gain could be made for subsequent recordings. In addition, monitor oscilloscopes were connected to each tape recorder channel so that signatures could be watched.

Time synchronization was handled by a Flow Corporation time code generator which occupied one tape recorder channel. The remaining data channel on the Ampex recorder was used for wind speed and direction information.

The apparatus for the static operation measurements was carried inside a battery-powered golf cart. Since the power to the vehicle was completely off while the vehicle was stopped, no electrical or audible interference was possible while helicopter hover recordings were being made. Instrumentation for these measurements (Figure 8b) consisted of a B&K 4145 1-in. (25.4-mm) condenser microphone boom-mounted on the end of a 6-ft (1.8-m) pole. The microphone was powered by a

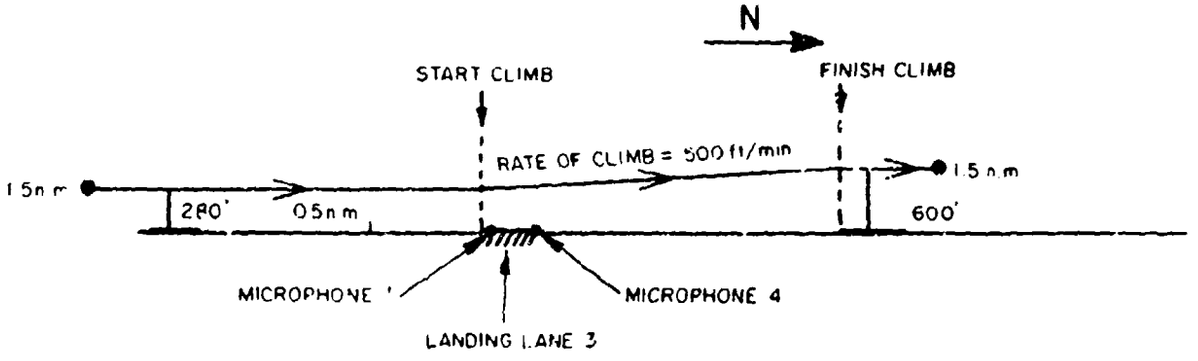

Figure 2. Flight path for first ascent.

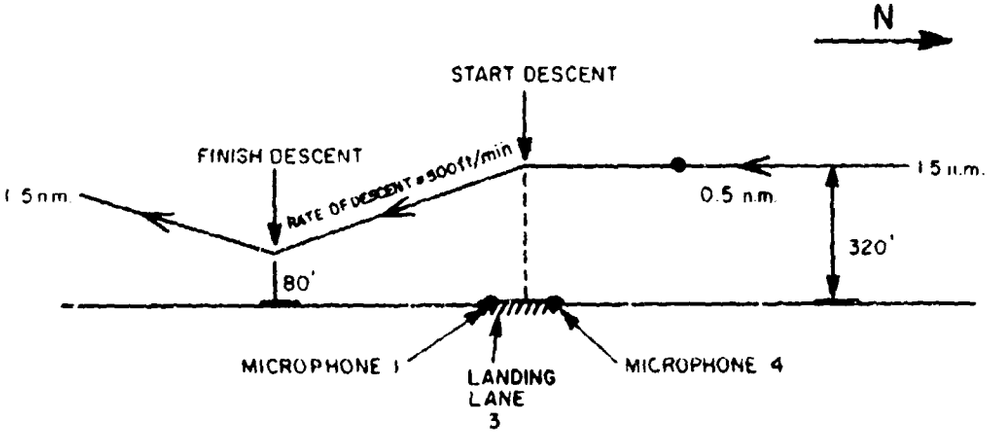

Figure 3. Flight path for first descent.

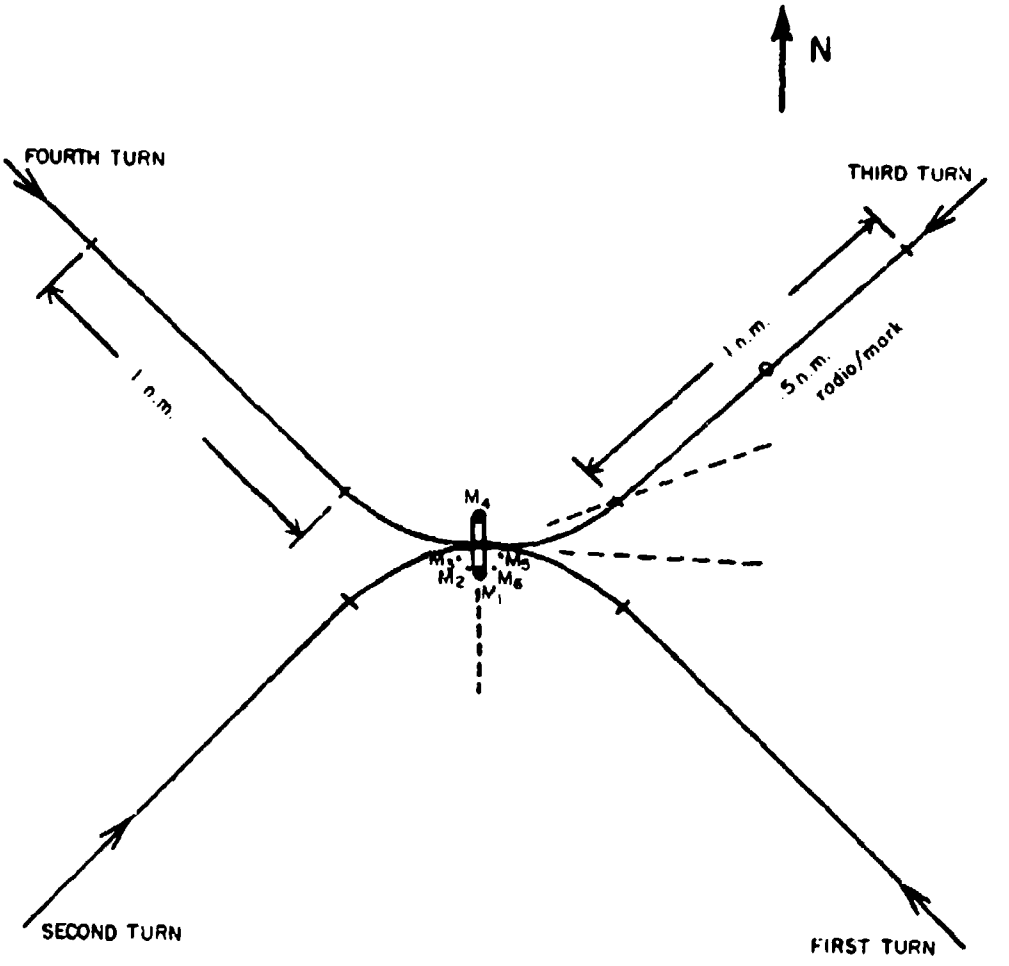

Figure 4. Flight path for 90-degree turns at 30-degree bank angles.

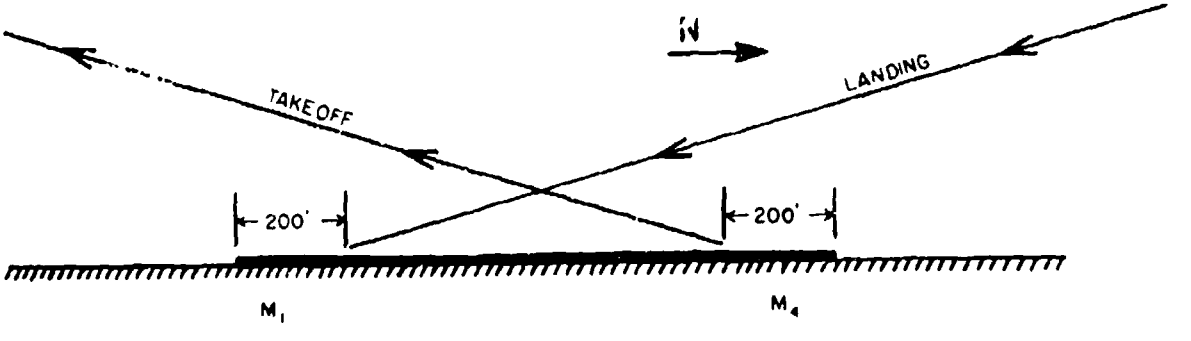

Figure 5. Flight path for takeoff and landing.

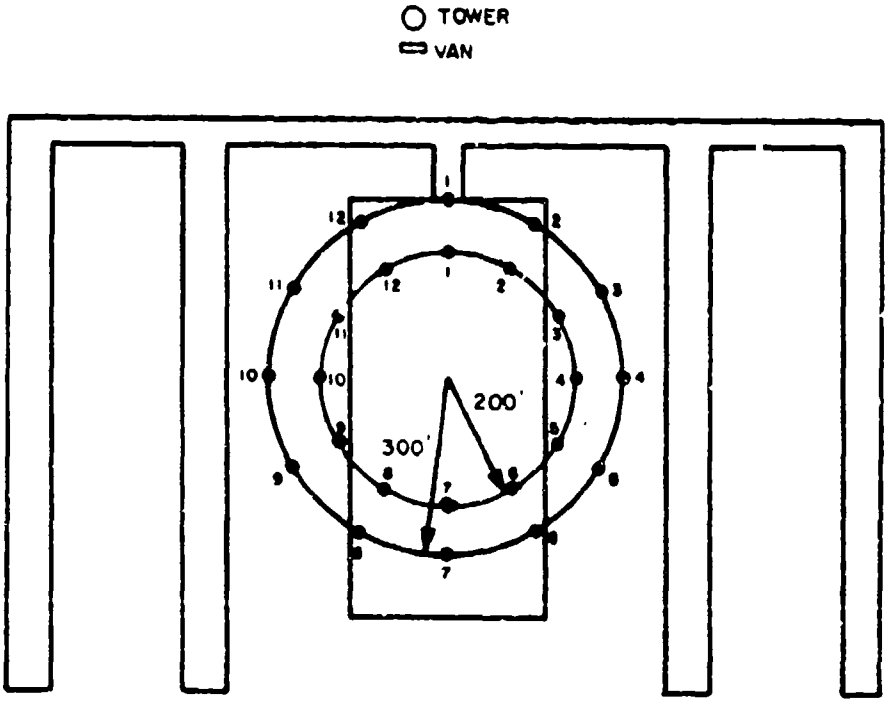

Figure 6. Setup for hover measurements showing measurement positions for in-ground and out-of-ground effect hovers.

B&K 2804 microphone power supply. This microphone's signal passed through a switch which was used to mark individual recordings by preceding them with the absence of a signal. The signal was split at this point between a monitor B&K 2209 sound level meter and three Nagra DJ full-track portable scientific tape recorders.

For in-ground effect hovers, the recorder designated as "A" in Figure 8b was set to run at 7.5 ips (191 mm/sec). The two speeds allowed for greater dynamic range in recording. Because of limited recording time at 7.5 ips (191 mm/sec) (i.e., the "A" recorder ran out of tape), another recorder ("C") running at 7.5 ips (191 mm/sec) was used in addition to the "B" recorder for the out-of-ground hover.

In-ground and out-of-ground effect hover measurements were performed around the aircraft at 30-degree angular intervals using 30-sec height-averaging measurements. The operator performed the height-averaging measurements by moving the boom-mounted microphone up and down in the vertical plane between 2 and 6 ft (0.6 and 1.8 m) above the ground. Height-averaging measurements were used when possible standing waves were to be negated. Upon completion of the measurements at one location, the microphone operator and electric golf cart moved to the next measurement position along the circle enclosing the aircraft.

Ground Tracking System

Making acoustical measurements of aircraft requires that position information be known. This information can be determined by elaborate radar tracking systems involving detailed and lengthy data reduction, or by much simpler systems.

The tracking system in this study consisted of two slaved cameras, three camera positions, and a theodolite (Figure 7). Camera 2 remained at the end of the runway (adjacent to microphone 4). The other camera was used in either position C_1 or C_3 depending on the angle

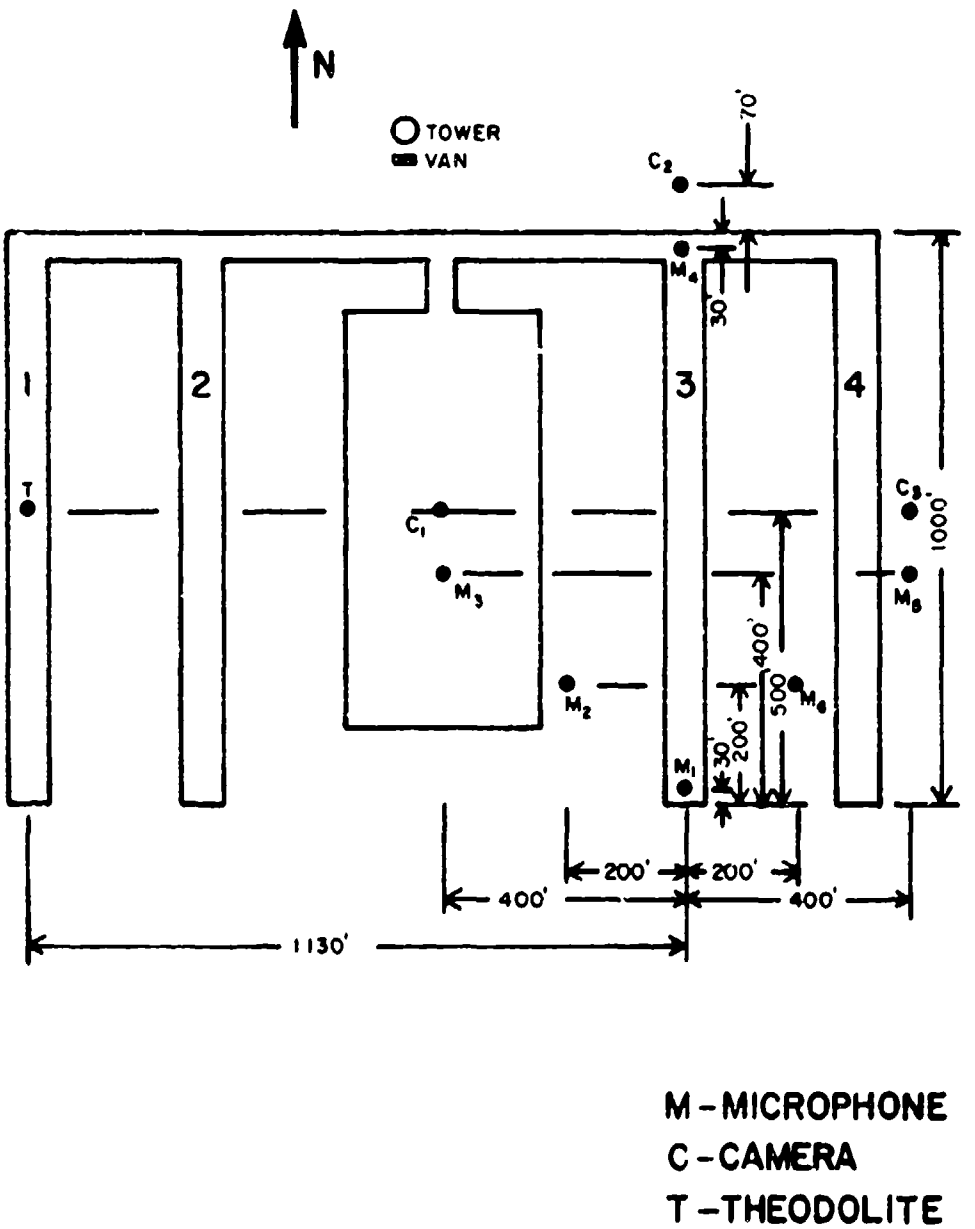

Figure 7. Equipment layout.

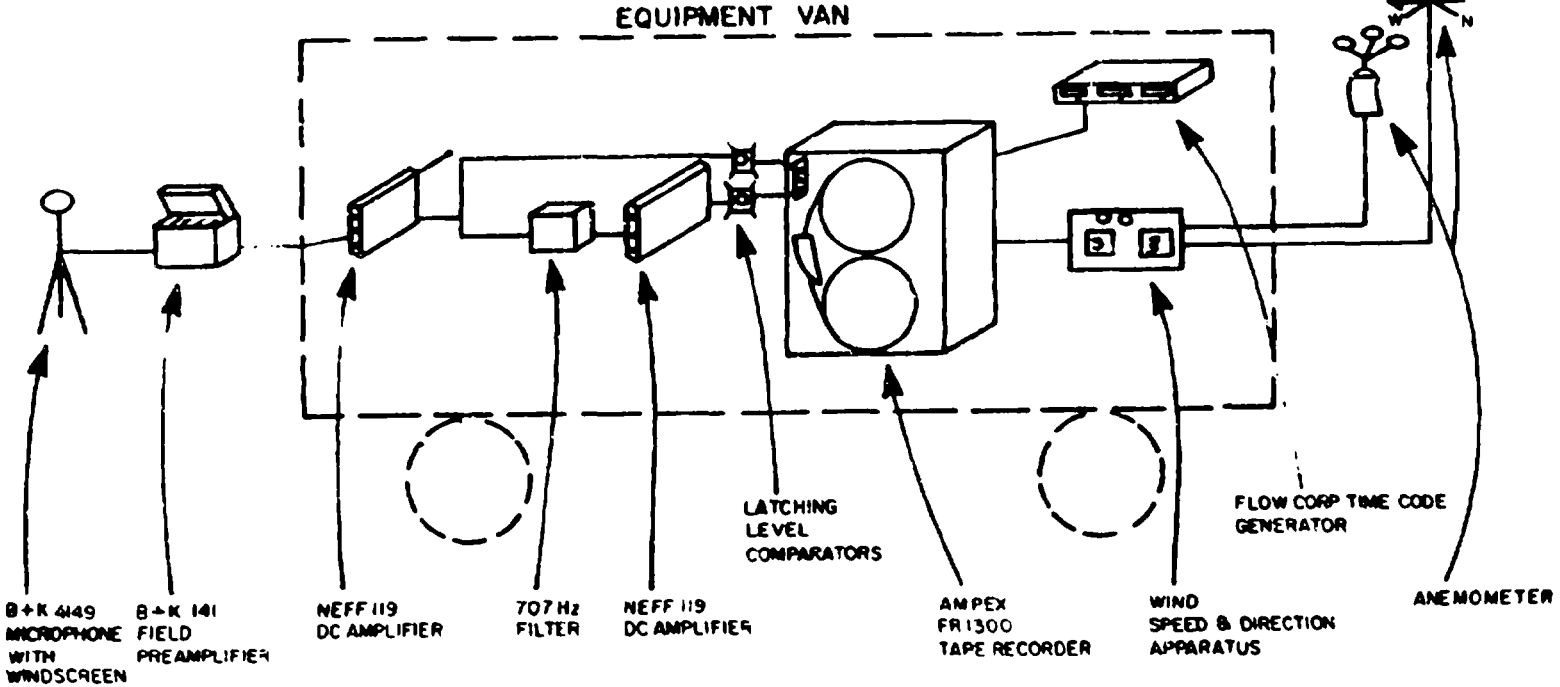

Figure 8. Measurement apparatus.

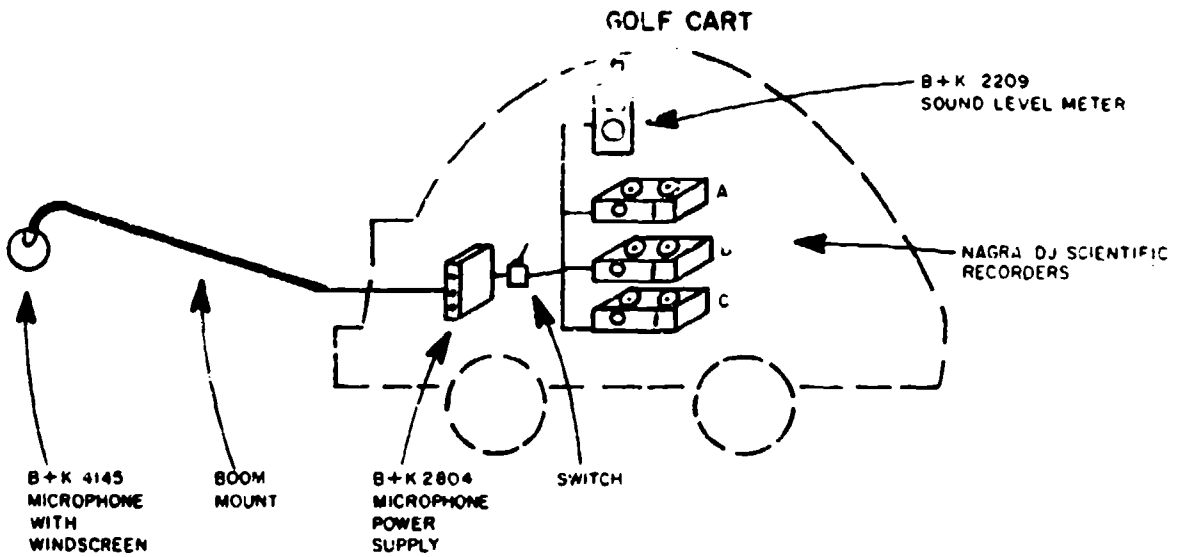

Figure 8. (cont'd)

of the sun. Stator poles located in front of camera positions were marked with uniform graduations. Position information in three dimensions could thus be ascertained at the moment that pictures were taken by examining photographs from both cameras. The theodolite served a go/no-go function to indicate whether the aircraft was within position limits.

A four-wire bus system connected the cameras with the van and the theodolite. When a picture was taken from either camera, both cameras were fired, wind direction information on the Ampex 14-track tape recorder was interrupted momentarily, and a tone was sounded at the theodolite. A push-button activator at the theodolite interrupted wind speed information on the Ampex recorder and sounded a tone at the control center. Photographs were taken when the aircraft was over the center of the landing lane, except during takeoffs and landings. In these cases, photographs were taken when the aircraft reached the end of the landing lane.

Calibration

Two types of calibration were performed for the dynamic operation array system. The first, a major electrical calibration and test, was done at the beginning of each day. An acoustical calibration was done at the beginning of every reel of tape for the Ampex recorder.

At the start of each day, the Ampex FR 1300 was aligned, and the wind speed and direction apparatus was calibrated. An electrical check was performed on the microphone system by injecting two square waves separately (low and high frequency) into the cathode follower of each channel. Response was checked with an oscilloscope.

At the beginning of each reel of tape, a B&K 4220 124-dB pistonphone was applied to the system with microphones in place, and k-factors were adjusted. Two of the six microphones were calibrated at a time, and the calibration information was recorded on magnetic tape. After acoustic calibration was complete, 1 minute of ambient noise was recorded.

The instrumentation for the static operation measurements was calibrated using a B&K 4220 pistonphone. The calibration tone was recorded onto all three Nagra recorders simultaneously. One minute of ambient noise was recorded after calibration was complete.

3 DATA REDUCTION

Raw Data

Each reel of tape from the 14-track Ampex FR-1300 tape recorder contained 12 channels of acoustical data: one channel of time code information; one channel onto which wind speed, wind direction, and signals from the cameras and theodolite were recorded; and one edge track onto which voice information was placed. Each reel of tape contained one set which consisted of 14 dynamic operations (runs) for each aircraft; there was a total of 40 sets (reels of tape).*

The 12 channels of acoustical data originated from the six microphones in the dynamic operations array. Each microphone signal was split: one part recorded linearly on one channel and the other sent through a 707-Hz high-pass filter and recorded on another channel. The object of this configuration was to prevent overloading or saturation of the electronics by the low-frequency components of the helicopter spectrum.

Time code information was supplied by a Flow Corporation time code generator. Day of the year, hours, minutes, and seconds were recorded on one channel of the Ampex recorder in digital format.

The remaining data channel contained the outputs of two voltage-controlled oscillators. These units were set up in such a way as to form a discrete frequency band for both. The voltage-controlled oscillators were driven by an R. M. Young wind speed and direction measurement apparatus. In this way, this tape channel could be read by a spectrum analyzer and wind speed and direction components ascertained. In addition, push-button activators (which were used to fire the camera bus) deleted the wind direction signal when pressed. The push-button activator at the theodolite momentarily interrupted the wind speed signal. The edge track contained a vocal running diary of events.

*Nineteen additional sets were recorded in a similar fashion for Navy and Marine helicopters at Camp Pendleton, CA.

Each operation (run) was photographed when the aircraft passed over the center of the landing lane as described previously. Two cameras 90 degrees apart focused on a point above the center of the runway where it was anticipated that the helicopter would fly. In the foreground of each photograph was a stator rod marked with uniform divisions. When the helicopter passed over the appropriate spot, an operator fired one of the cameras. A four-wire bus system fired the other camera and at the same time momentarily interrupted the wind direction signal as described above.

Each photograph carried position information in the form of altitude and side-to-side variation. The time at which the photographs were shot was noted on the analog recording.

In addition, a written record was kept by the theodolite operator. Since the theodolite was fixed in place for each run, the operator could record the relative altitude of the helicopter in the field of view when the cameras were fired (and a Sonalert near the theodolite sounded). The theodolite was only used to check results from the cameras.

Reduction of Dynamic Operation Data

The most economically feasible method was sought for capturing data from tape while at the same time maintaining a high dynamic range. Since the Federal Scientific UA-14A 400-line spectrum analyzer had a lower dynamic range than the Ampex FR 1300 tape recorder, it was decided that two passes of each tape recorder channel would have to be performed at differing gains to match the dynamic range of the tape recorder. A Nova 1200 minicomputer sampled the spectrum analyzer every 0.5 sec, summed the spectra into one-third octaves, and stored the contents on disk. Since each microphone signal was split while recording (one high frequency and one low frequency channel), a total of four passes was performed for each of the six microphones.

The procedure for the two-pass system was as follows. At first detection of a helicopter, the tape and analysis equipment were started. The first pass was made with a high gain setting. Some overloading of the spectrum analyzer was expected, and these portions were flagged by the minicomputer. After the helicopter being analyzed was no longer detectable, analysis stopped, the tape was rewound, and gain to the analyzer was lowered in preparation for the second pass. For record-keeping purposes, the minicomputer was used interactively; that is, information was requested from

the operator before and after each pass. For the second low gain pass, the analysis was started at the same time on tape by use of the time code channel in order to insure synchronization between the passes. The two passes were meshed by incorporating data from the second low gain pass whenever it was indicated that the high gain pass was overloaded. This same procedure was repeated for the other channel of the low-high frequency pair for each microphone, and results fitted together to form the full spectrum per 0.5 sec for each microphone.

Reduction of data from the two cameras was handled differently. Since a graduated stator rod was present in the foreground of each photograph, altitude and side-to-side variation over the center of the landing lane could be read if the camera angle, distance to the stator rod, and distance between graduations on the stator rod were known. Corrections were made for aberrations in the lens.

Negatives of each helicopter were projected on the screen of a microfiche reader, measurements were taken in relation to the stator rod, and data were encoded into the minicomputer for further calculation and analysis. Algorithms were written that located the helicopter in three dimensions at the time both cameras were fired, given the information supplied in the two pictures. The slant distance to each of the six microphones in the array was calculated based on the position of the helicopter in space.

The problem of different types of noise being present is inherent in any analysis procedure. Noise from different sources only becomes significant when it approaches the signal level. Numerous methods are available to ascertain the combined noise level; some of these will be discussed here.

It is important that when noise readings are taken, gain settings throughout the system remain the same as they were when the helicopter data were recorded. For the first noise reading–ambient noise–a recording was made immediately after the helicopter left the area following a set. This reading reflected ambient sounds (such as wind, vehicles, birds, and other environmental sounds) that occurred while tests were in progress.

Electrical noise–the noise of the system that is constant at different gain settings–was measured by attaching a dummy microphone to the cathode follower at one of the stations and measuring the resultant level on playback from tape.

The third noise reading--tape noise–was taken by shorting the input to one channel and recording. On playback, the level was measured.

The three noise levels were summed to calculate a composite noise level (CNL) by one-third octaves for each gain setting used. The correct CNL was compared to the resultant one-third octave spectra for each 0.5 sec, and those 0.5-sec intervals were flagged if their levels came within 3 dB of the CNL value.

Reduction of Static Operation Data

Reduction of the hover data was performed in two steps. First, a polar plot was made of the data for each helicopter under each unique condition such as normal or maximum loading or in-ground or out-of-ground effect hover. Comparing these data for different helicopters of the same type under similar conditions indicated substantial variability in the individual L_{eq} values (plus or minus 5 dB). These variations were observed during the actual recording of data and resulted primarily from pilot actions as the hovering helicopter was kept at a constant altitude and facing into a variable wind.

Because of the large variability in the data for an individual helicopter, it was decided to form average polar plots for all of the helicopters (except the CH-47 and CH-54 which were measured at 300 ft [91 m] instead of 200 ft [61 m] as were the other six aircraft).

4 DATA ANALYSIS

As indicated in Chapter 3, dynamic operation data were reduced into one-third octave spectra for each 0.5 sec of recording. Essentially, the analysis of these reduced data took two steps:

1. Calculation of the integrated A-weighted sound exposure level (SEL) for each microphone recording.

2. Development of A-weighted SEL versus distance relations.

Step 1 has two parts. First, the A-weighted SEL was calculated for the microphone flyover. Essentially, this calculation involves forming the integral of the A-weighted pressure squared received by the microphone. The 0.5-sec time interval having the maximum A-weighted value was determined, and the entire one-third octave spectrum for that 0.5 sec was recorded. The dis-

tance of closest approach from aircraft to microphone for each individual flyover recording at each microphone was determined from the positional information recorded photographically and synchronized to the magnetic tape recording. The maximum spectrum and distance of closest approach were then used to convert the raw SEL (A-weighted) to an equivalent SEL for a day with a standard temperature of 59°F (15°C) and relative humidity of 70 percent.

In the second step, A-weighted SEL versus distance relations were established. The data used were the SEL at the microphone corrected to the standard day conditions, the distance of closest approach from aircraft to microphone, and the maximum and one-third octave spectra during the half-second having the maximum A-weighted reading. Distance causes three factors to vary: (1) air absorption (the one-third octave spectrum was used to determine the effect of air absorption); (2) the $1/r^2$ amplitude change of a point acoustical source; and (3) the apparent durational change of a source moving in a straight line at constant speed. Since all Army helicopters operate at about the same speed, speed was not considered in this analysis. Appendix A contains a detailed description of this analysis procedure, which is structured similarly to the Air Force procedure[7] that was written in part to describe the reduction of fixed-wing aircraft data. The primary difference between the Air Force and Army data reductions is that the Air Force used tone corrections and effective perceived noise level (EPNdB) as well as A-weighted levels. The Joint Services (in conjunction with DOD) subsequently agreed to eliminate EPNdB in lieu of A-weighted levels and to eliminate the tone corrections. Additionally, it was found that the concept of tone correction did not apply to helicopters since the primary noise source is the rotor rather than the engines.)

Three methods were employed to test the sensitivity and validity of the Air Force's data reduction method. Two of these methods used an alternate spectrum instead of the spectrum during the 0.5 sec having the maximum A-weighted level. In one case, the average spectrum over the entire recording of an individual flyover was employed and in the other, a normalized spectrum for the entire flyover was formed by treating each 0.5 sec as equal. Since it is the spectrum which, along with distance, is used to convert the raw data to average day and to account for air absorption, it was felt that these alternate spectra would indicate any significant problems. Typically, use of either of these alternate spectra results in SELs which agree within a few tenths of a decibel with the Air Force method over all of the distances for which SEL was calculated.

As an even more rigorous test, SEL values were calculated by reconstituting the noise produced by the helicopter as it traveled along its flight path and attenuating the reconstituted noise to the various points (distances) at which one wanted to calculate SEL. Because of the finite length of actual recording, this process could only be accurate to distances of about 10,000 ft (3 km). Within this distance constraint, the more complicated process described above was found to agree within about 1 dB or less with the simpler method employed by the Air Force for data reduction.

On the basis of the three alternate data reduction methods described above, the best procedure for Army use was determined to be the Air Force method; this method was selected so that all of DOD's aircraft data would be reduced using essentially the same procedure.

Analysis of the hover data was quite simple. It should be recalled that a 3-sec recording was made at 30-degree increments around the hovering helicopter at a distance of 200 ft (61 m) from the center of the helicopter (300 ft [91 m] for the CH-47 and CH-54 helicopters). Analysis consisted of direct measurement of the equivalent levels (L_{eq}) A-weighted for each 30-sec recording. This L_{eq} measurement was performed using the CERL True Integrating Noise Monitor and Sound Exposure Level Meter (which employs a true integrating detector).

5 EXPLANATION OF DYNAMIC OPERATIONS SEL CURVES AND STATIC OPERATIONS L_{eq} PLOTS

Combination of Dynamic Operations

Once SEL vs distance values had been generated, these data had to be combined into a form usable in the field. The Nova 1200 minicomputer was the logical choice for analysis, since interactive operation was possible.

The minicomputer provided a number of options, including combining, printing, and plotting data. A brief description of the combining options is presented here.

[7] D. E. Bishop and W. J. Galloway, *Community Noise Exposure Resulting from Aircraft Operations: Acquisition and Analysis of Aircraft Noise and Performance Data*, Report AMRL-TR-73-107 (BBN, 1975).

For any particular run, the user was given a choice of data specification. One method allowed set, operation, and microphone number to be specified for combining. The other method allowed the user to choose aircraft, loading conditions, operations, and wind/microphone relations. This method will be described here.

For any particular run, the user was asked to select one or more aircraft for the run and, if applicable, whether these aircraft were to have normal and/or maximum loading. One or more operations was selected next: level flight, ascent, descent, takeoff, landing, or turns. Next, for mean wind velocity, the user could select one or more of the four bands between 0 and 20 knots (617 m/sec) in 5 knot (154/m sec) increments, greater than 20 knots (617 m/sec), or all wind velocities. One or more wind velocity standard deviations were available to the user. Wind/microphone relations were also available so that the user could select the wind direction (head, tail, port, or starboard) and the microphone relation (upwind and downwind for head and tail, sideline [upwind and downwind] and beneath for port and starboard).

After some computation, the SEL vs distance tables shown in Appendix B were developed.

Analysis of SEL vs Distance Curves

Operations Distant From Airfields

The first group of plots in this section provides SEL vs distance curves for cross-country flying and other maneuvers performed distant from airfields, heliports, and landing pads. Operations considered are level flyovers, ascents, descents, and turns. For each SEL vs distance plot presented in this section, Appendix B also provides the corresponding set and operation numbers used to form the plot.

Figure 9 presents all aircraft (with both normal and maximum loading) grouped according to operation. Inspection reveals that level flyovers and turns are coincident. Compared to these, descents are approximately 1.5 dB higher, and ascents are about 1 dB lower. Level flyovers and turns are expected to be the same, since inside and outside turns* were considered. When inside and outside turns are separated and plotted against level flyovers (Figure 10), it is seen that outside turns are, at the most, 1.5 dB higher than inside turns. When ascents and descents (combined) are plotted against level flyovers (Figure 11), ascents and descents exceed level flyovers by only 0.5 dB. It can therefore be concluded that level flyovers, inside and outside turns (combined), and ascents and descents (combined) produce nearly coincident curves. Since the resultant values from level flyovers, ascents, and descents are all similar, differences under loading conditions were examined. Figures 12 and 13 show the CH-47, CH-54, UH-1H, and UH-1B aircraft plotted under normal and maximum loading conditions for level flyovers and ascents and descents (combined). From these plots, the differences between the two conditions are found to be 1.5 dB for CH-54s, 1 dB for UH-1Hs, 0 dB for CH-47s, and 0 dB for UH-1Bs.

Figure 14 shows the eight Army models tested with normal and maximum loading combined on those aircraft so tested. In this plot, the aircraft fall into four groups:

Group 1: CH-47

Group 2: CH-54, UH-1H, AH-1G

Group 3: UH-1B, UH-1M

Group 4: OH-58, TH-55.

Figure 15 compares these four groupings to all aircraft.

There are not enough data to substantiate sufficiently the quantitative results for wind effects in level flyovers, ascents, and descents. Qualitative trends, however, may be drawn.

Figure 16 shows curves with respect to wind direction (head, tail, port, and starboard). Here, only data corresponding to winds within ±15 degrees of each primary direction were considered; data represented by the other 240 degrees were excluded from the analysis. It is noted that data gathered with port and starboard winds are close to one another as are data gathered with head and tail winds.

Figure 17 depicts combined data for head and tail winds and port and starboard winds. On this plot, level flyovers (winds from 360 degrees considered) are shown as a reference. These data indicate that on the

*For inside and outside turns, only microphones 1 and 4 (at opposite ends of runway 3) were used for analysis. Inside turns are defined as those 3 degree/sec, 90-degree turns in which the subject microphone sees a concave flight path. Conversely, the subject microphone views a convex flight path for outside turns.

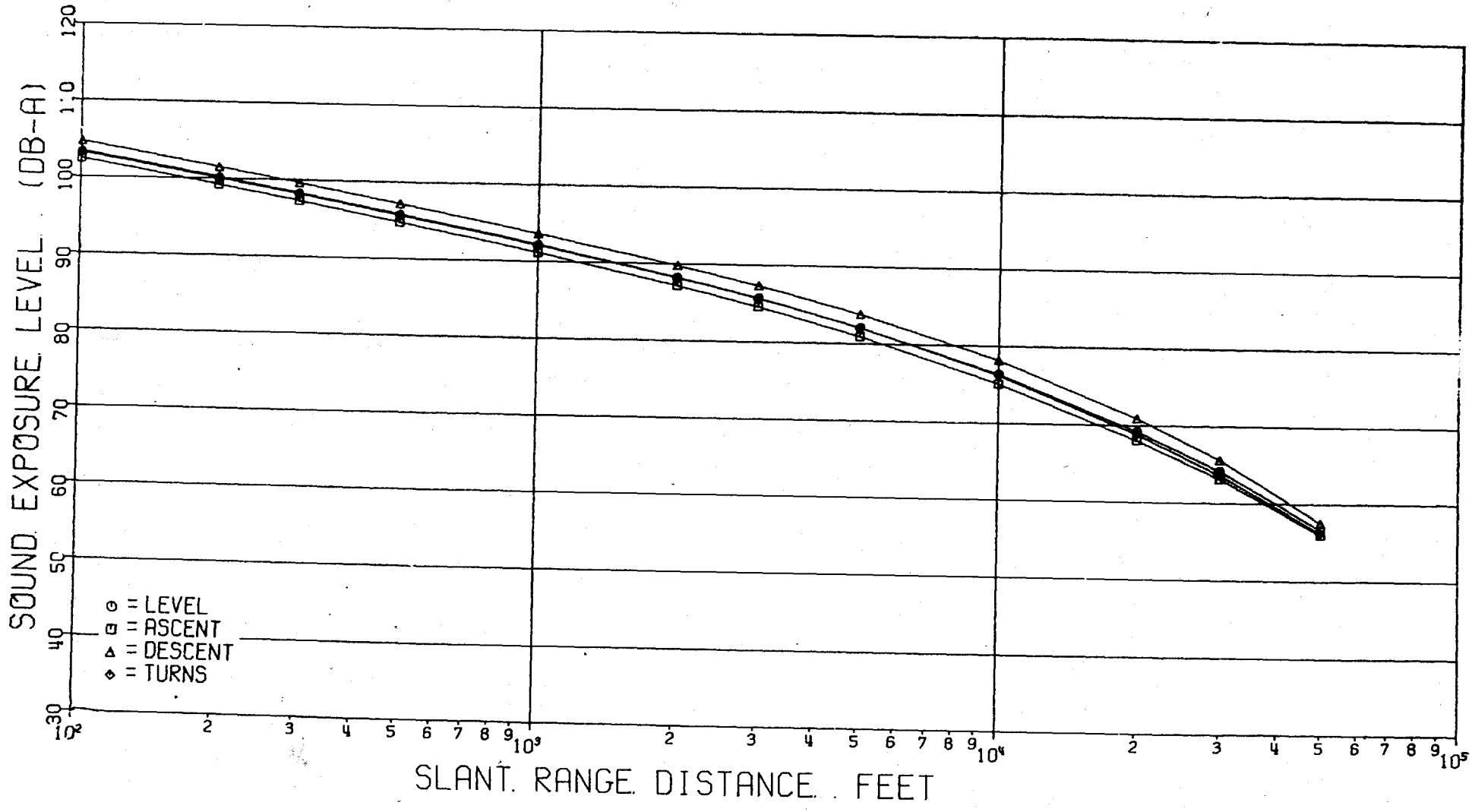

Figure 9. SEL vs distance curves for all aircraft grouped according to operation. SI conversion factor: 1 ft = 0.3048 m.

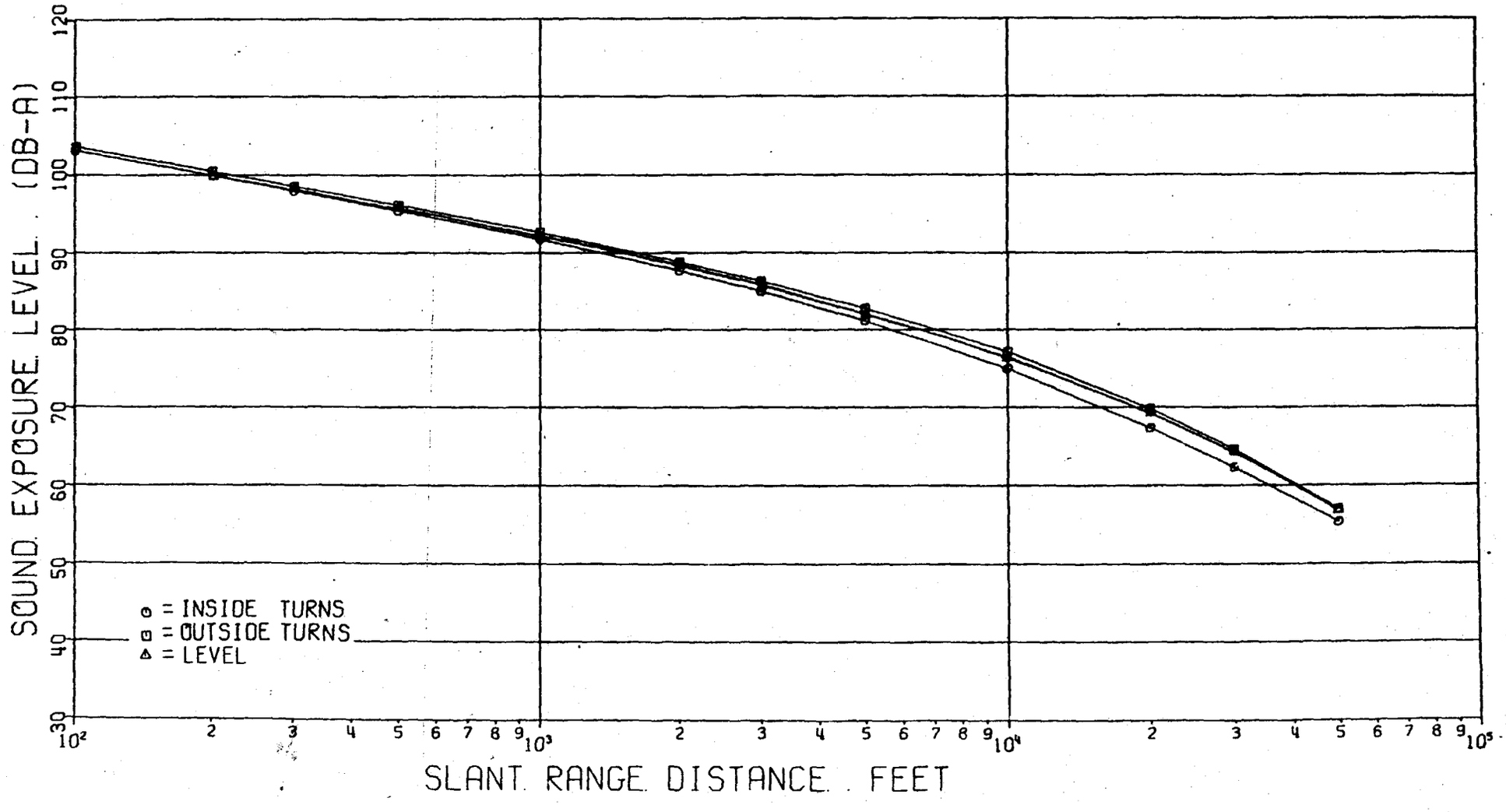

Figure 10. SEL vs distance curves for inside and outside turns (separate) compared to level flyovers. SI conversion factor: 1 ft = 0.3048 m.

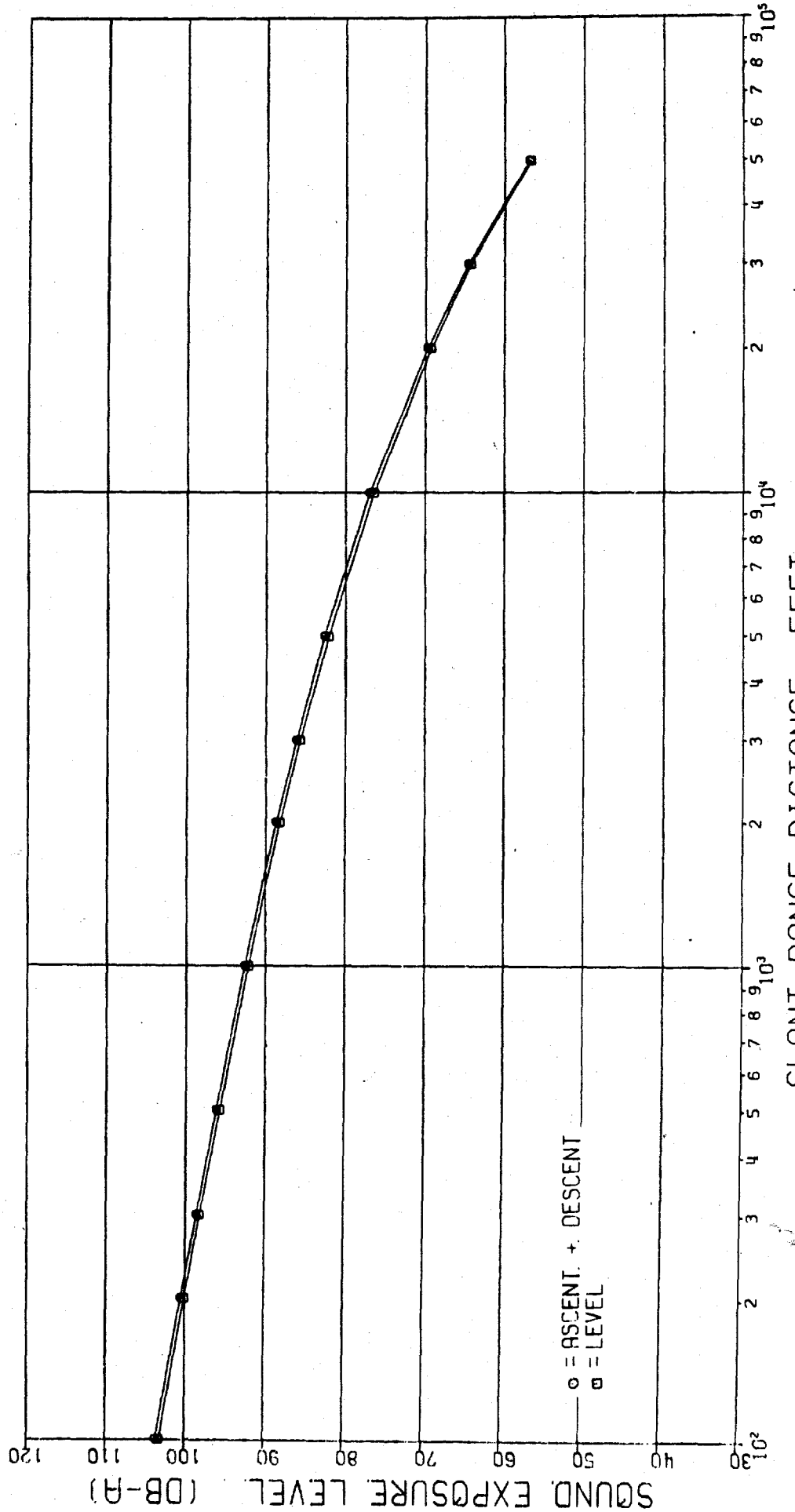

Figure 11. SEL vs distance curve for ascents and descents (combined) compared to level flyovers. *SI* conversion factor: 1 ft = 0.3048 m.

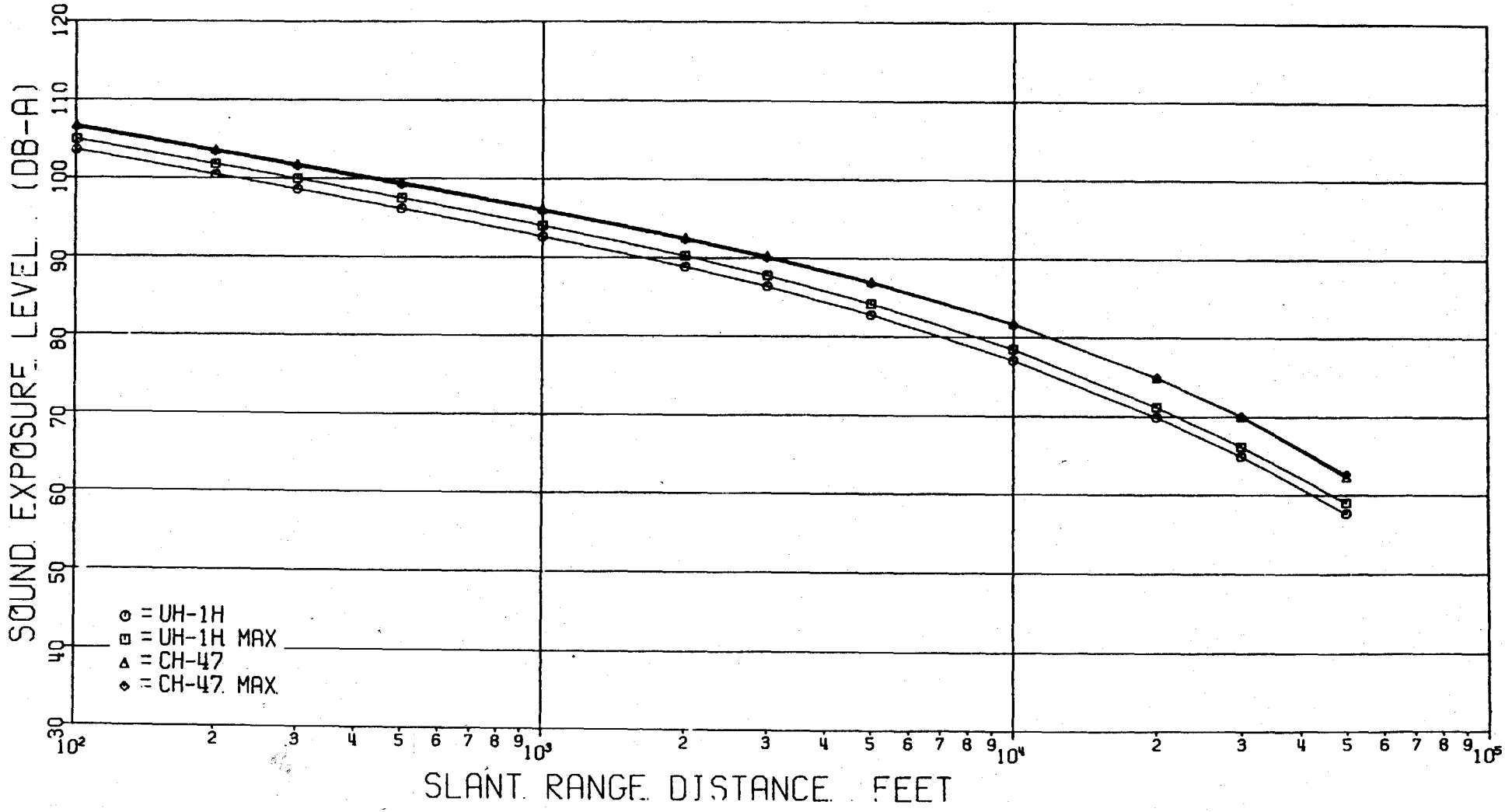

Figure 12. Comparison of normal and maximum loading for UH-1H and CH-47 aircraft. SI conversion factor: 1 ft = 0.3048 m.

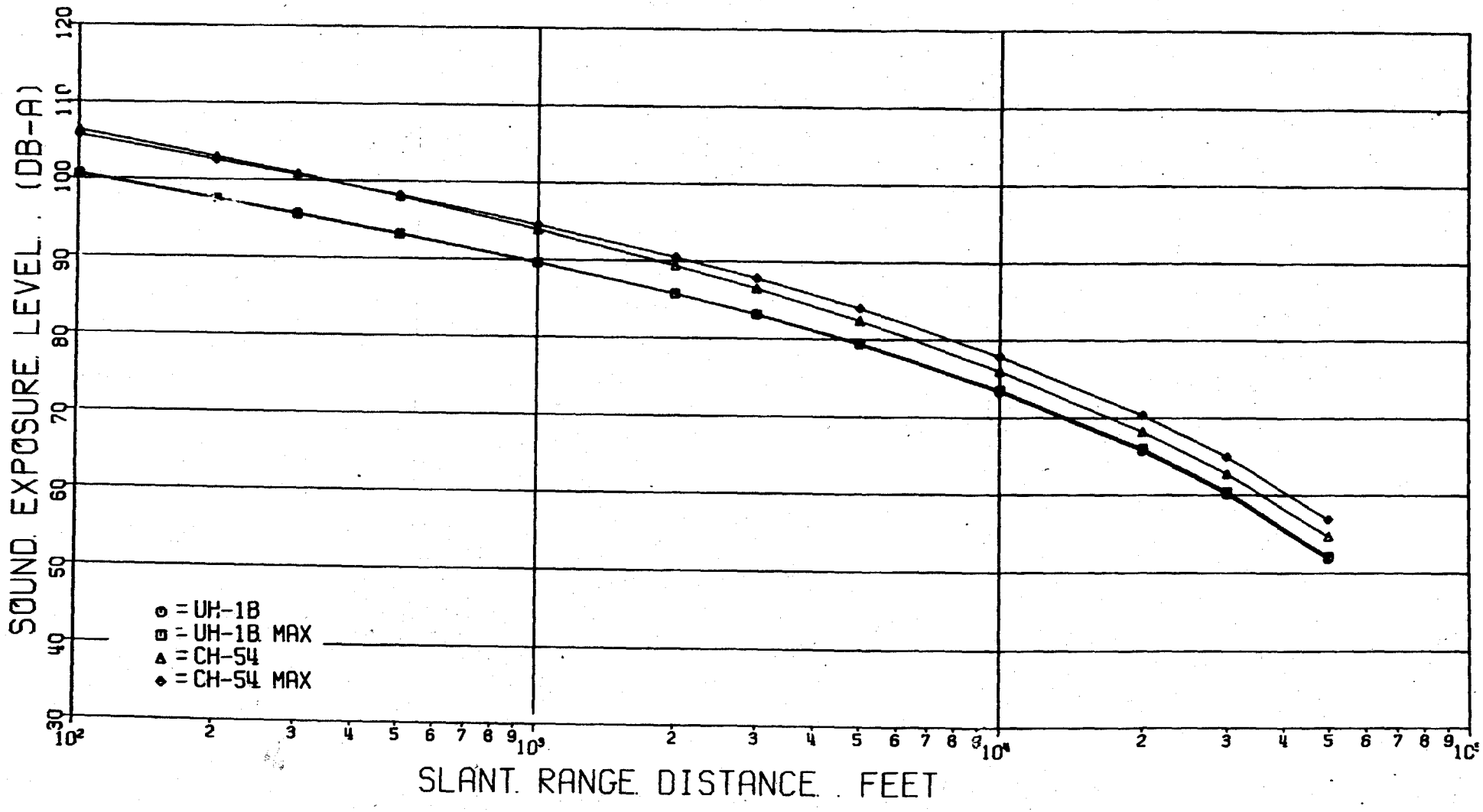

Figure 13. Comparison of normal and maximum loading for UH-1B and CH-54 aircraft. SI conversion factor: 1 ft = 0.3048 m.

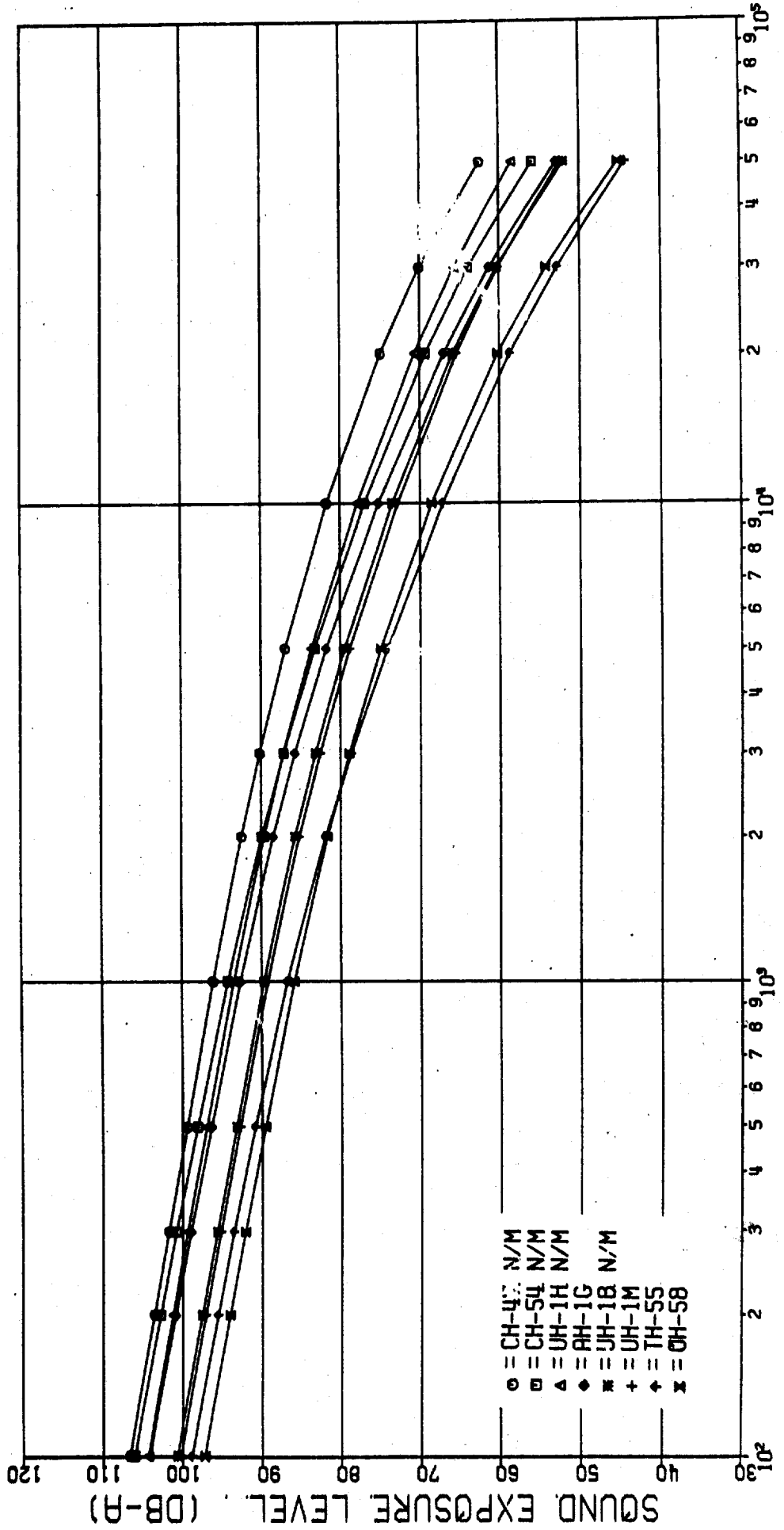

Figure 14. Combined loadings for eight aircraft tested.
SI conversion factor: 1 ft = 0.3048 m.

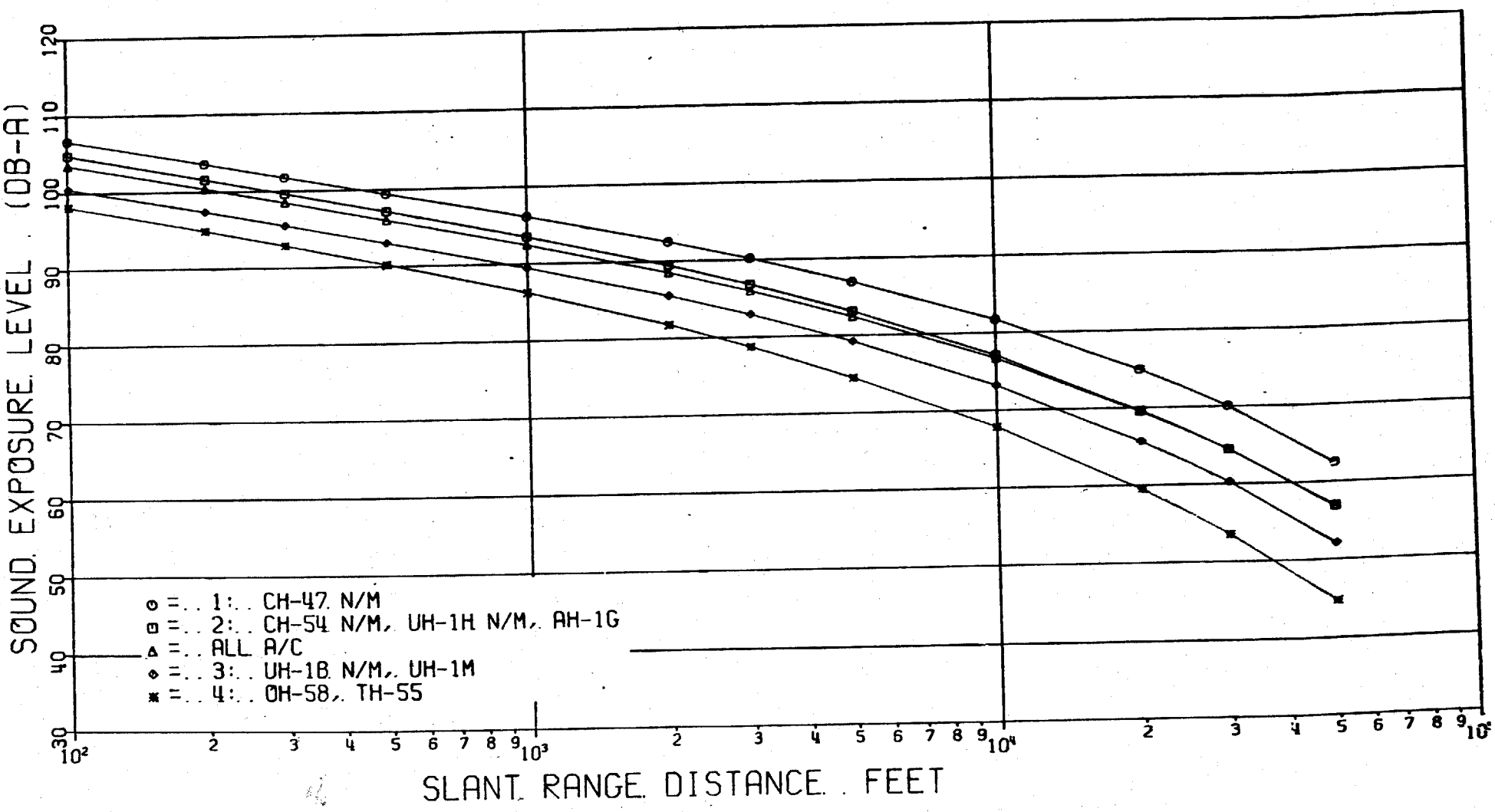

Figure 15. Four groupings of aircraft compared to level flyovers.
SI conversion factor: 1 ft = 0.3048 m.

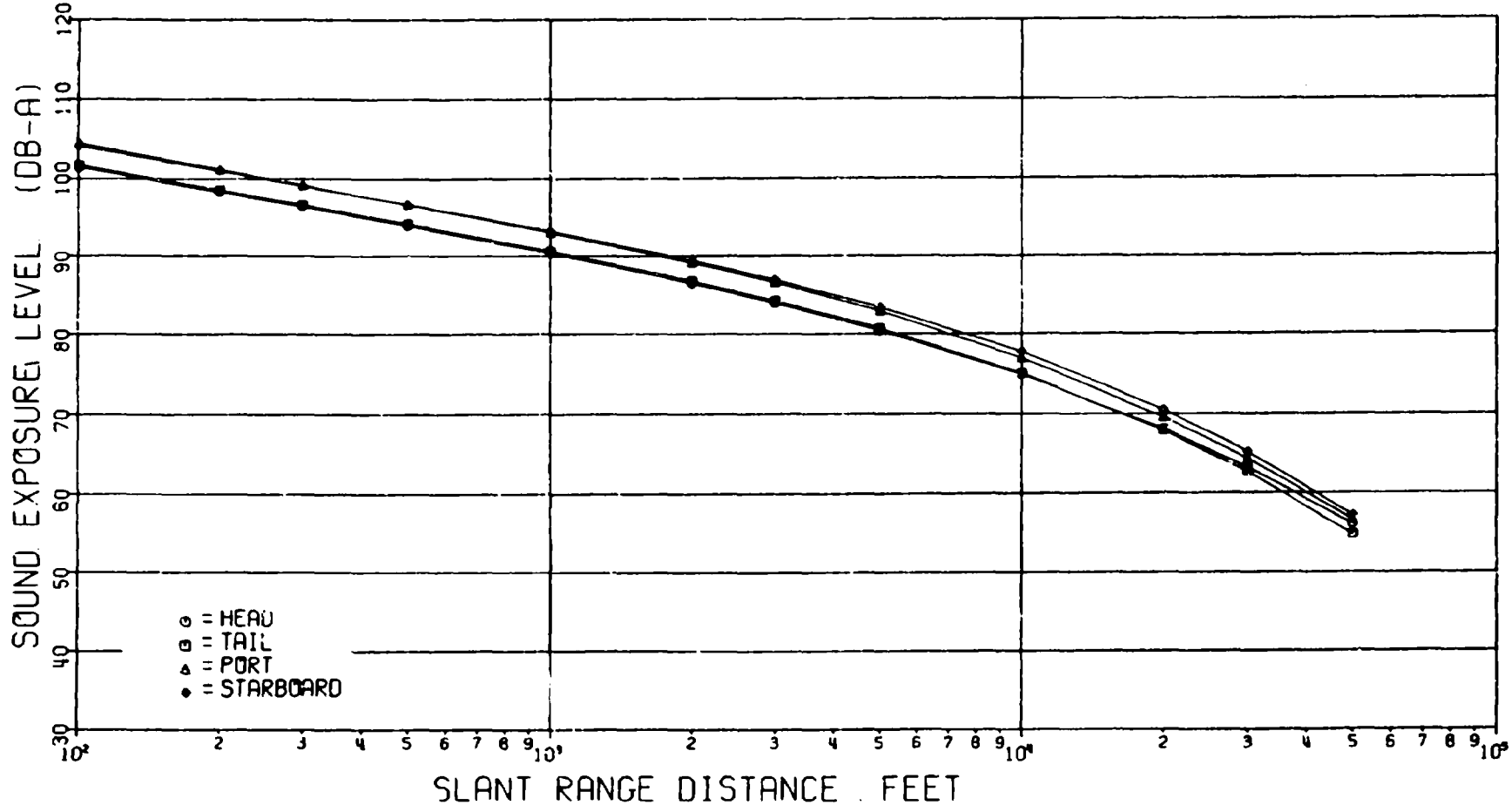

Figure 16. SEL curves with respect to wind directions.

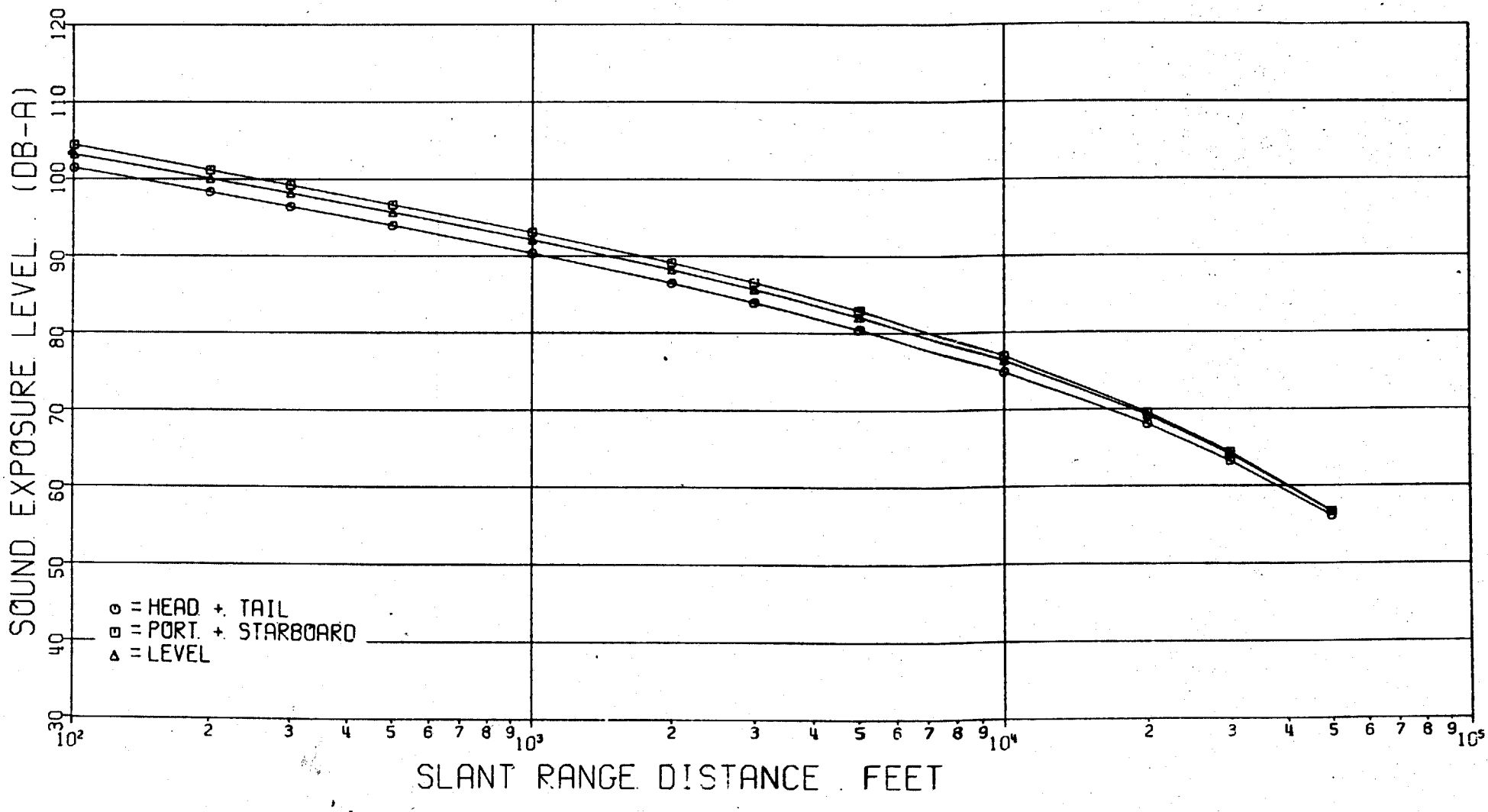

Figure 17. Combined data for head and tail winds (combined) and port and starboard winds (combined). SI conversion factor: 1 ft = 0.3048 m.

average, wind is not a factor and that variation is less than 1 to 2 dB. There were not enough data to compare up and down wind situations because the site was layed out to maximize head and tail wind conditions.

Figure 18 presents data corresponding to wind speed. Data are plotted in increments of 5 knots (154 m/sec). Here, SEL values are monotonically decreasing with increasing speed range plotted.

Figure 19 shows differences between data recorded on sideline microphones and data recorded on microphones beneath the flight path. Data recorded on sideline microphones were about 1.5 dB lower than data recorded on microphones directly beneath the flight path for level flyovers and ascents and descents combined.

Operations Proximate to Airfields

Figure 20 presents SEL curves for landings. Here, the data are grouped into two sets of sideline microphones and one microphone located in front of the aircraft (see Figure 7 for microphone position). As a reference, level flyovers are also plotted. These curves show that aircraft are typically louder to the front than to the sidelines when landing and that landings are louder than level flyovers.

Figure 21, which shows all landing microphones combined vs level flyovers, indicates that SEL values for landings are typically 3 to 5 dB higher than those for level flyovers. This factor is suitable for use in manual predictions.

Figure 22 shows data grouped by microphones for takeoffs compared to level flyovers. Only microphone 4 is significantly different from a level flyover; this difference was caused by the fact that the helicopter hovered before taking off. This hover period must be treated in an analogous fashion to ground run-ups for fixed-wing aircraft. Figure 23 gives the directivity pattern to apply and Table 3 corrects the pattern to absolute levels for individual aircraft. Appendix C provides directivity patterns (L_{eq} plots) for in-ground and out-of-ground effect hovers for each type of aircraft tested. The flight portion of takeoffs is adequately approximated by level flyovers.

Combination of Static Operations Data

As explained in Chapter 3, because of the large variability in the data for an individual helicopter, average polar plots were formed for all of the helicopters (except the CH-47 and CH-54, which were measured at 300 ft [91 m] instead of 200 ft [61 m] as were the other aircraft).

Figure 9 shows these average polar plots for in-ground and out-of-ground effect hover conditions. All of the data for the different aircraft were first normalized to 80 dB so that these polar plots would not be dominated by the larger helicopters. Table 3 lists the correction factor necessary to scale the normalized polar plots back to an actual polar plot for each of the individual aircraft at a reference distance of 200 ft (61 m).

6 CONCLUSIONS AND RECOMMENDATIONS

Conclusions

This report has provided state-of-the-art Sound Exposure Level (SEL) versus distance curves (Figures 9 through 22) with supporting operational information (Appendix B) for eight models of Army rotary-wing aircraft. Equivalent Sound Level (L_{eq}) contours for hovering aircraft are also furnished (Figure 9, Table 3, Appendix C). Data as presented are suitable for use in either manual or computerized techniques for the prediction of noise impact from rotary-wing aircraft.

The following conclusions can be drawn about the data presented here:

1. The same levels (coincident SEL vs distance curves) result from the following operations for all aircraft:

   a. Level flyovers

   b. Inside and outside turns combined

   c. Ascents and descents combined

Since the data are coincident, the noise impact may be adequately described by using the level flyover SEL vs distance data shown in Figure 9 only.

2. The effect of having aircraft fully loaded (with troops, equipment, etc.) rather than normally loaded is slight and may be ignored (Figures 12 and 13).

Table 3
Correction Factor Necessary to Scale Normalized Polar Plots to Actual Plots for Each Individual Aircraft

Measurement Angle (in Degrees)	OH-58		AH-1G		UH-1B	
	In-Ground	Out-of-Ground	In-Ground	Out-of-Ground	In-Ground	Out-of-Ground
0	-1.2	-4.0	11.8	-8.8	-7.5	-6.2
30	1.4	-5.1	12.0	-10.1	-4.7	6.4
60	0	-5.7	8.7	-11.9	-4.6	7.5
90	-2.6	-6.0	7.8	-9.4	-4.0	8.4
120	.4	3.5	-4.7	-9.7	-6.8	11.7
150	.5	1.0	5.2	-8.9	-5.0	-11.3
180	2.2	2.1	7.4	-5.6	3.9	8.3
210	.6	.3	7.3	-2.0	-6.1	10.3
240	1.8	3.7	7.6	-2.5	-6.3	13.0
270	-4.7	-2.1	-9.9	-8.1	-7.4	-8.0
300	-1.8	-8.5	-10.9	-10.1	-9.4	-10.0
330	-1.3	-6.1	-11.1	-6.6	-5.8	-8.4

Measurement Angle (in Degrees)	UH-1M (Normal and Maximum Loading)		UH-1H (Normal and Maximum Loading)		TH-55
	In-Ground	Out-of-Ground	In-Ground	Out-of-Ground	
0	-8.3	-7.3	-9.0	-9.5	-1.1
30	8.3	-9.7	6.2	8.1	-3.9
60	5.6	9.8	-6.4	9.7	-3.0
90	4.6	12.3	-4.6	10.2	-4.2
120	5.4	11.0	6.3	10.8	4.4
150	4.0	7.9	9.2	14.2	7.2
180	6.7	10.4	10.6	13.2	3.4
210	6.0	10.8	9.6	13.5	4.6
240	5.5	9.4	-7.3	11.3	6.6
270	6.7	-10.6	-7.6	-8.3	-3.9
300	10.1	10.5	-10.1	10.8	-4.3
330	7.8	-8.1	-8.6	-8.9	-1.4

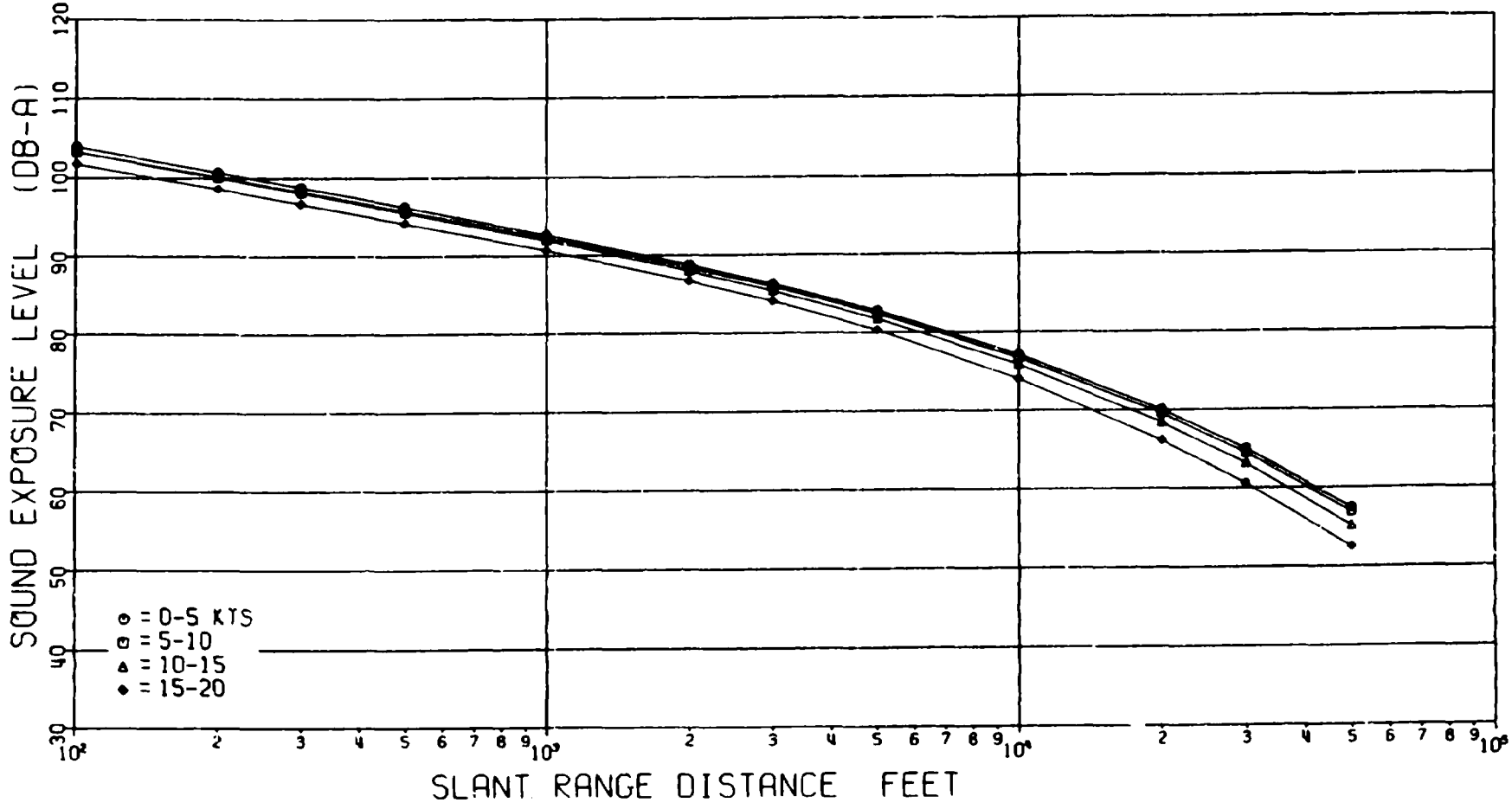

Figure 18. Data corresponding to wind speed. SI conversion factor:
1 ft = 0.3048 m; 1 knot = 30.87 m/sec.

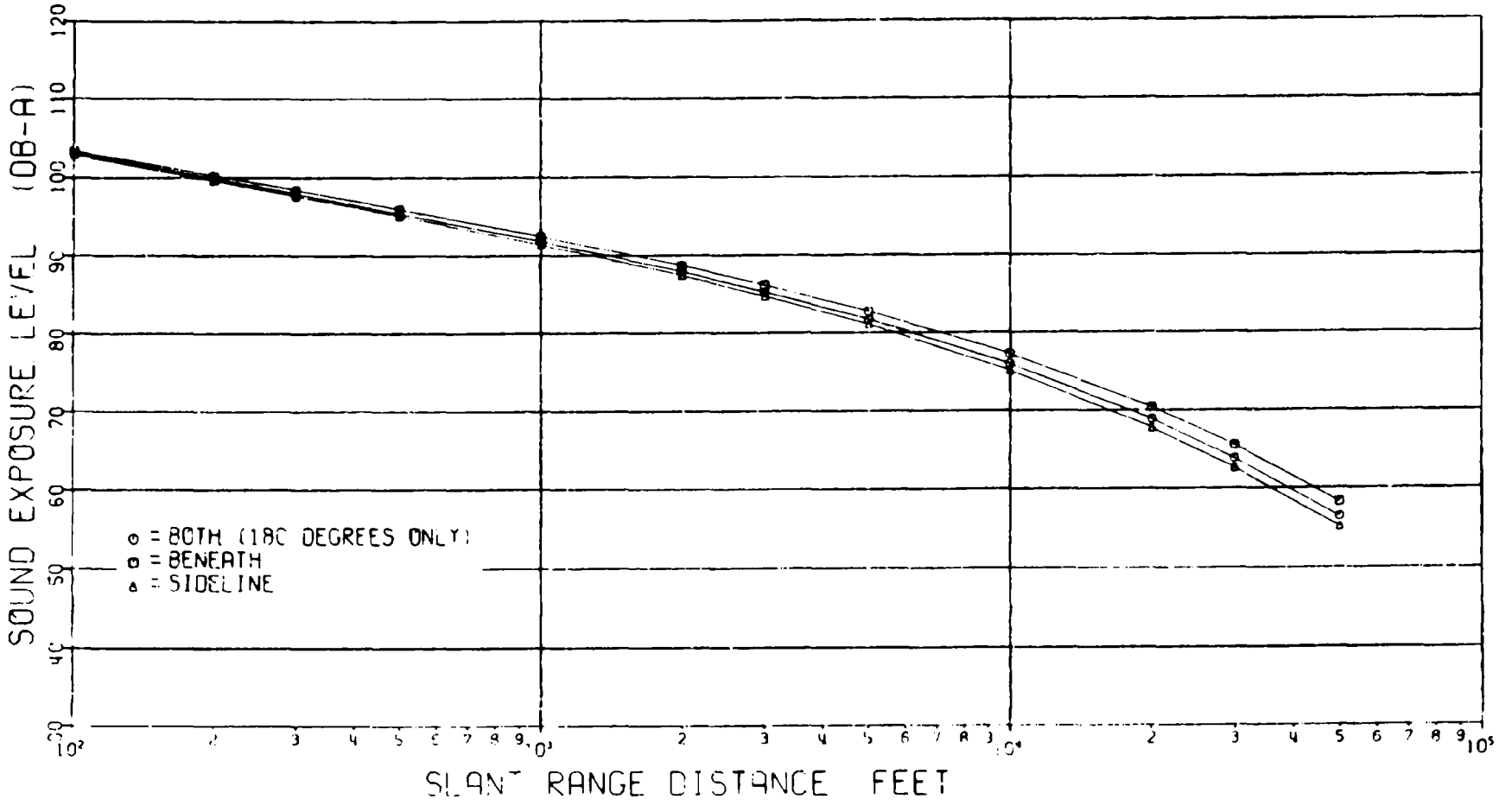

Figure 19. Difference between data recorded on sideline microphones and microphones beneath flight path. SI conversion factor: 1 ft = 0.3048 m.

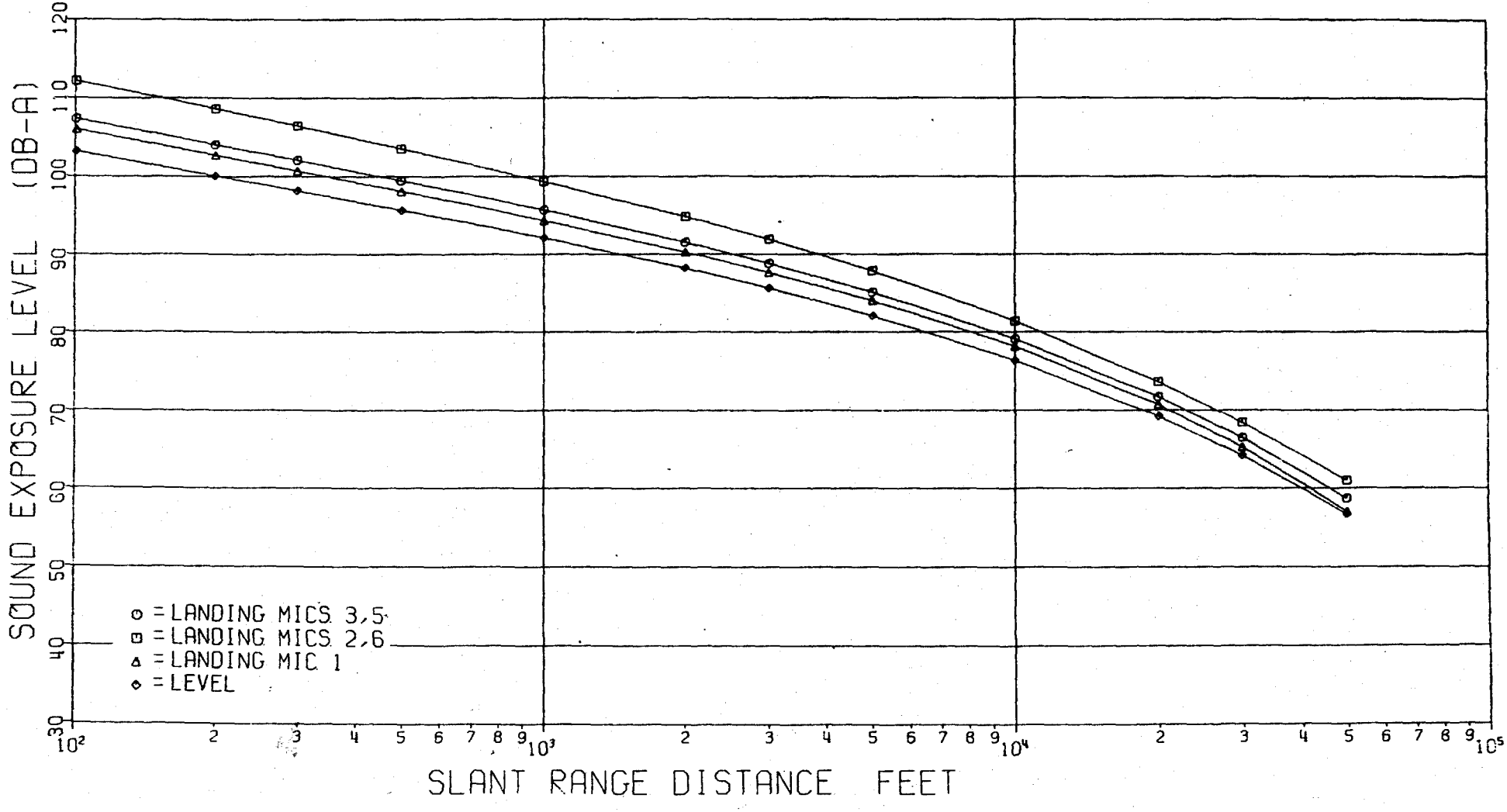

Figure 20. SEL curves for landings grouped by microphones.
SI conversion factor: 1 ft = 0.3048 m.

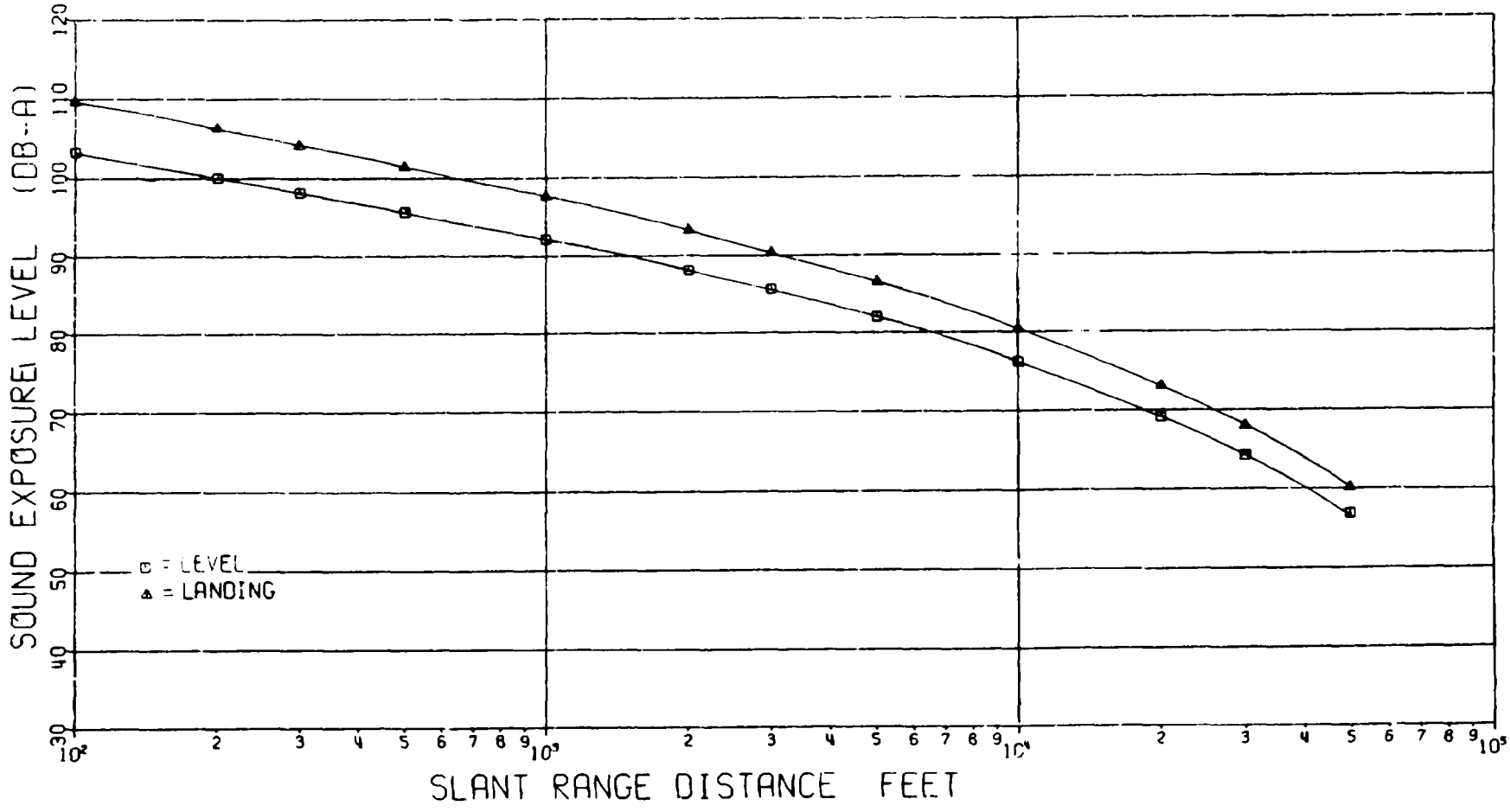

Figure 21. All landing microphones (combined) compared to level flyovers. SI conversion factor: 1 ft = 0.3048 m.

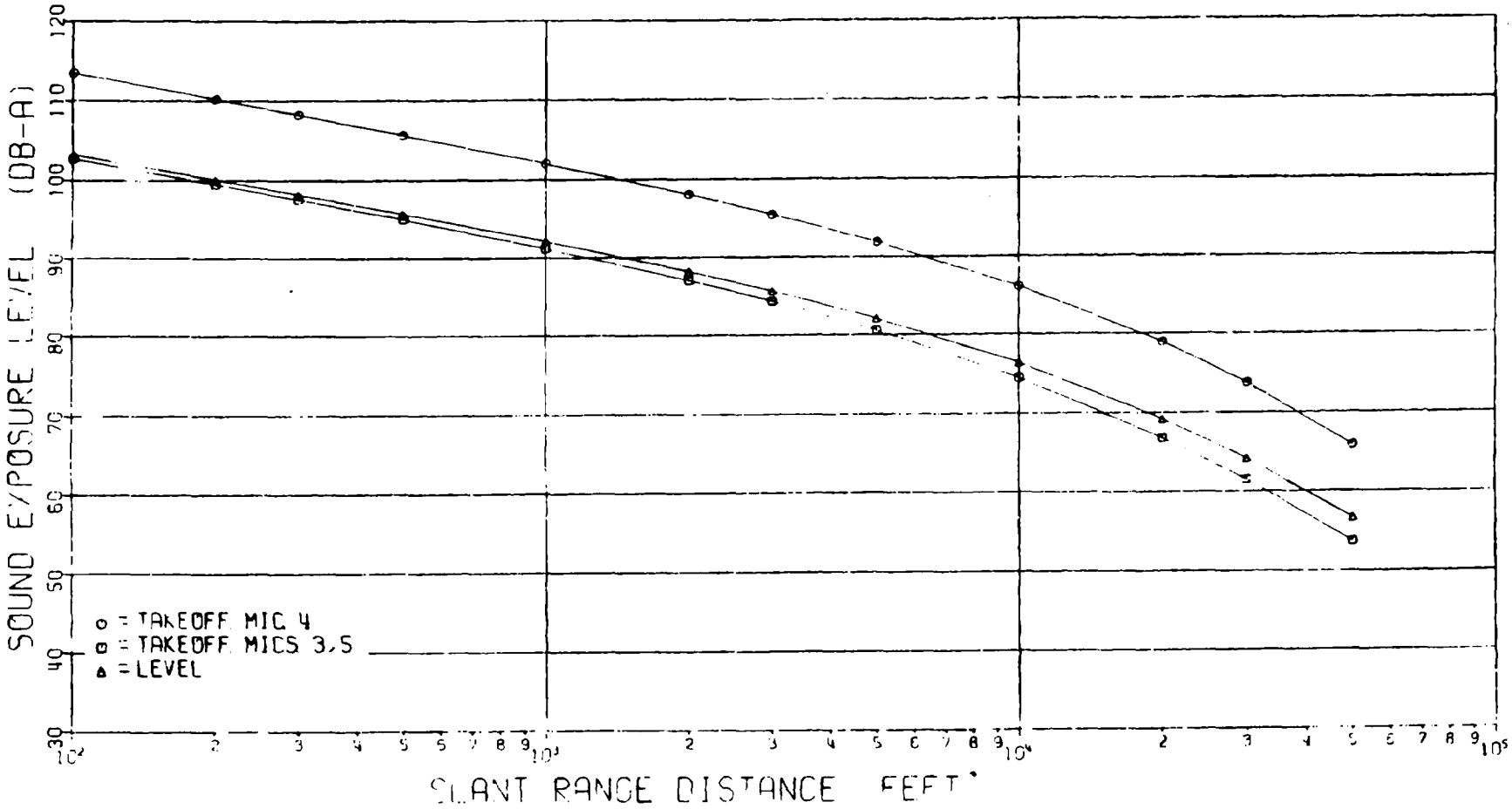

Figure 22. SEL curves for takeoffs grouped by microphones.
SI conversion factor: 1 ft = 0.3048 m.

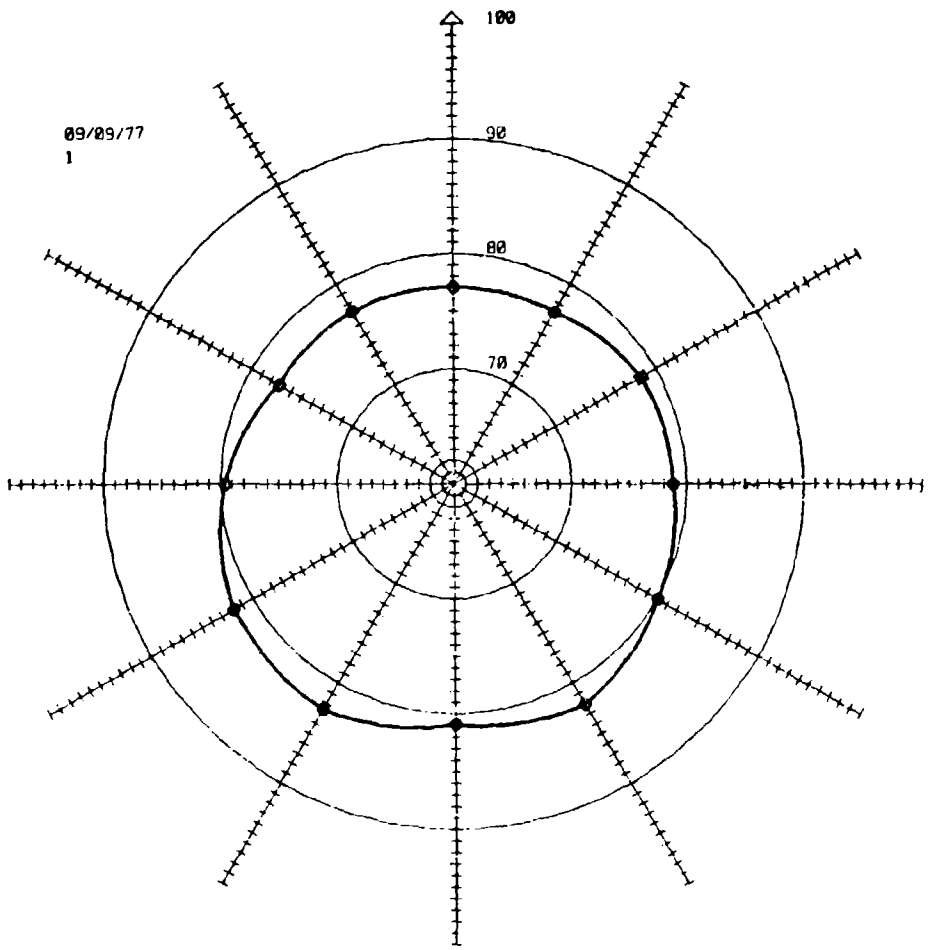

Measurement Position:	0°	30°	60°	90°	120°	150°	180°	210°	240°	270°	300°	330°
L_{eq}:	77.0	77.2	78.5	78.8	80.1	82.1	80.9	82.7	81.8	79.6	77.2	77.3

Figure 23. Average polar plots for in-ground and out-of-ground effect hover conditions normalized to 80 dB for all aircraft except CH-47 and CH-54.

3. For bases having a large number of aircraft of any particular model type, a grouping may be chosen to more closely reflect the actual noise impact (Figure 15).

4. The effects of wind direction are small and tend to cancel each other (Figure 17).

5. Measured noise levels decrease with increasing wind velocity (Figure 18).

6. A direct overflight is somewhat noisier than a sideline flyover for the same slant distance (Figure 19).

7. Landing aircraft produce higher noise to the front than the sides (Figure 20).

8. Landings produce SEL levels approximately 3 to 5 dB higher than level flyovers (Figures 20 and 21).

9. Aircraft preparing to take off produce higher SEL levels than they do during takeoffs (Figure 22). These "ground run-ups" may be predicted using in-ground effect hover data (Figure 23 and Table 3).

10. Once off the ground, takeoffs may be approximated by the level flyover curve (Figure 22).

Recommendations

It is recommended that the state-of-the-art data presented in this report be used in any manual and computerized techniques used to predict noise impact for Army rotary-wing aircraft. When these data are included in an automated (computerized) prediction system, it is recommended that:

1. When predicting the noise impact from a single aircraft, the level flyover or combined level flyovers, ascents, and descents data be used (Figure 14).

2. When predicting impact for a fleet of aircraft, individual groupings (Figure 15) be used.

3. When landing direction is known, Figure 20 be used to allow for high levels in front of the aircraft.

When performing manual predictions, it is recommended that the curve for all aircraft in Figure 15 be used. This curve is weighted toward UH-1s; since the Army's fleet of rotary-wing aircraft is similarly weighted, this curve is realistic in most cases.

REFERENCES

Air Installations Compatible Use Zones, DOD Instruction 4165-57 (Department of Defense, 1973).

Bishop, D. E. and W. J. Galloway, *Community Noise Exposure Resulting From Aircraft Operations: Acquisition and Analysis of Aircraft Noise and Performance Data*, Report AMRL-TR-73-107 (Bolt, Beranek and Newman [BBN], 1975).

Construction Criteria Manual, DOD 4270.1-M (Department of Defense, 1972).

Horonjeff, R. D., et al., *Community Noise Exposure Resulting from Aircraft Operations: Computer Program Description*, Report AD/A-004821 (Bolt, Beranek and Newman [BBN], 1974).

Schomer, P. D. and B. L. Homans, *User Manual: Interim Procedure for Planning Rotary-Wing Aircraft Traffic Patterns and Siting Noise-Sensitive Land Uses*, Interim Report N-10/ADA031450 (U.S. Army Construction Engineering Research Laboratory [CERL], 1976).

APPENDIX A:

DESCRIPTION OF ANALYSIS PROCEDURE

Symbols

Subscripts

1. A subscript "f" indicates a noise measurement obtained in the field without adjustment to reference conditions.

2. A subscript "j" indicates a running index associated with measurements on specific flights, where "j" indicates the flight number.

3. The subscript "i" is a running index associated with any one band in the set of one-third octave frequency bands.

4. A variable with a superscript apostrophe (read as "prime") identifies a value of the variable intermediate in the process of determining the final value adjusted to reference conditions.

5. A subscript "r" indicates the value of a variable at its reference condition.

Acoustical

AL — A-weighted sound level, in dBA, as specified in IEC Publication No. 179.

ALM — Maximum A-level occurring during a noise event.

dB — Decibel.

ASEL — Sound exposure level, in dB, is the level of the time-integrated mean square A-weighted sound pressure for an event, with a reference time of one second:

$$\text{ASEL} = 10 \log \int_{-\infty}^{+\infty} 10^{\frac{AL}{10}} dt$$

For purposes of aircraft noise evaluation, SEL is computed from A-levels sampled at discrete intervals of 0.5 sec or less. Thus the working expression for SEL becomes:

$$\text{ASEL} = 10 \log \sum_{k=0}^{k=\frac{d}{t}} 10^{\frac{AL(k)}{10}} + 10 \log \Delta t$$

where d is the time interval during which AL(k) is within 10 dB of the maximum A-level, and Δt is the time interval between noise level samples.

SPL — Sound pressure level in dB.

α — Sound attenuation coefficient in air.

Δ — Adjustment factors to reduce test conditions to reference conditions.

Geometry

L — Point of receiver.

Q — Point on flight path closest to point L.

S — Distance from point L to point Q.

x — Arbitrary slant distance.

Computation of ASEL Versus Distance Curves From Level Flyover Noise Measurements—Air-to-Ground Propagation

It is assumed that ASEL is the sum of the A-level maximum (ALM) plus a duration correction, D(AL). It is further assumed that ASEL varies with distance because of:

a. Changes in ALM which are caused by inverse square changes in SPLs and changes in SPLs caused by air absorption.

b. Changes in D(AL) which are directly proportional to air speed* and inversely proportional to distance.

It is also assumed that ALM is generated at an angle of maximum radiation, θ.

Normalization of Level Flyover Data to Standard Day Conditions and to Any Slant Distance

Develop basic description of noise levels as a function of aircraft performance from level flyovers. Adjust all flyover data to reference acoustical day conditions (59°F, 70 percent relative humidity) and distance x.

a. Obtain ASEL_{fj} (dB)

b. Obtain slant distance S_j from L to Q (ft)

*Since model-to-model variation in rotary-wing air speed is small, the effect of air speed can be ignored.

c. Compute $\alpha_i S_j$ for all i (ft)

d. Compute $\alpha_{ir} x$ for all i (where α_{ir} refers to sound attenuation coefficients for 59°F, 70 percent relative humidity). (dB)

e. Obtain $\Delta_{5j} = 20 \log_{10} \frac{S_j}{x}$ (dB)

f. Obtain $\Delta_{2j} = -10 \log_{10} \frac{S_j}{x}$ (dB)

g. Obtain $SPL'_{ij} = SPL(\theta)_{ij} + \alpha_i S_j - \alpha_{ir} x + \Delta_{5j} + \Delta_{2j}$ (where $SPL(\theta)_{ij}$ is the one-third octave SPL for ALM_j) (dB)

h. Compute AL'_j from SPL'_{ij}. (dB)

i. Obtain $ASEL_{xj} = ASEL_{ij} + AL'_j \quad ALM_j$ (dB)

APPENDIX B:

SEL TABLES FOR DYNAMIC OPERATIONS

This appendix contains 14 tables each having two parts. The first part of each table (a) presents SEL vs distance data for a particular case in tabular form; the second (b) shows which sets and runs are represented in the tables.

Table B1
Operation From Airfields–All Aircraft
(Normal and Maximum Loading)
a. SEL Values, dBA

Slant Distance ft	(m)	Level Flyovers	Ascents	Descents	Turns
100	(30.5)	103.1	102.3	104.6	103.3
200	(61.0)	100.0	99.1	101.4	100.1
300	(91.4)	98.1	97.2	99.5	98.2
500	(152.4)	95.6	94.7	97.1	95.7
1000	(304.8)	92.0	91.1	93.5	92.1
2000	(609.6)	88.1	87.1	89.7	88.2
3000	(914.4)	85.6	84.5	87.2	85.6
5000	(1524)	82.0	80.8	83.7	82.0
10000	(3048)	76.3	75.0	78.1	76.1
20000	(6096)	69.1	67.9	70.8	68.7
30000	(9144)	64.1	63.0	65.5	63.5
50000	(15240)	56.6	55.9	57.5	56.1
Data Points		446	461	448	292

Table B1 (Cont'd)
b. Set and Run Information

Set	Model	Max Load	Level 360	Level 180	Ascent 360	Descent 180	Descent 360	Ascent 180	LT from SE	RT from SW	RT from NE	LT from NW
	Operation											
1.	OH-58		1	1	2	3	3	2	4	4	4	4
2.	OH-58		1	1	2		3	2		4		
27.	OH-58		1	1	2	3	3	2	4	4	4	4
28.	OH-58		1	1	2	3	3	2	4	4	4	4
4.	AH-1G		1	1	2	3		2	4	4	4	4
5.	AH-1G		1	1	2	3	3	2	4	4	4	4
39.	AH-1G		1	1	2	3	3	2	4	4	4	4
40.	AH-1G		1	1	2	3	3	2	4	4	4	4
6.	UH-1M		1	1	2	3	3	2	4	4	4	4
13.	UH-1M		1	1	2	3	3	2	4	4	4	4
29.	UH-1M		1	1	2	3	3	2	4	4	4	4
30.	UH-1M		1	1	2	3	3	2	4	4	4	4
15.	UH-1H		1	1	2	3	3	2	4	4	4	4
17.	UH-1H		1	1	2	3	3	2	4	4	4	4
25.	UH-1H				2	3	3	2	4	4	4	4
33.	UH-1H		1	1	2	3	3	2	4	4	4	4
16.	UH-1H	X	1	1	2	3	3	2	4	4	4	4
18.	UH-1H	X	1	1	2	3	3	2	4	4	4	4
26.	UH-1H	X	1	1	2	3	3	2	4	4	4	4
34.	UH-1H	X	1	1	2	3	3	2	4	4	4	4
19.	UH-1B		1	1	2	3	3	2	4	4	4	4
21.	UH-1B		1	1	2	3	3	2	4	4	4	4
23.	UH-1B		1	1	2	3	3	2	4	4	4	4
20.	UH-1B	X	1	1	2	3	3	2	4	4	4	4
22.	UH-1B	X	1	1	2		3	2	4	4	4	4
24.	UH-1B	X	1	1	2	3	3	2	4	4	4	4
8.	CH-47		1	1	2	3	3	2	4	4	4	4
14.	CH-47		1	1	2	3	3	2	4	4	4	4
37.	CH-47		1	1	2	3	3	2	4	4	4	4
7	CH-47	X	1	1	2	3	3	2		4		4
38.	CH-47	X	1	1	2	3	3	2	4	4	4	4
9.	CH-54		1	1	2	3	3	2	4	4	4	4
11.	CH-54		1	1	2	3	3	2	4	4	4	4
10.	CH-54	X		1	2	3	3					
12.	CH-54	X	1	1	2	3	3	2	4	4	4	4
31.	TH-55		1	1	2	3	3	2	4	4	4	4
32.	TH-55		1	1	2	3	3	2	4	4	4	4
35.	TH-55		1	1	2	3	3	2	4	4	4	4
36.	TH-55		1	1	2	3	3	2	4	4	4	4

Key: 1 = Level flyovers
2 = Ascents
3 = Descents
4 = Turns

Table B2
Inside and Outside Turns – All Aircraft
(Normal and Maximum Loading)
a. SEL Values, dBA

Slant Distance ft	(m)	Inside Turns	Outside Turns
100	(30.5)	103.0	103.5
200	(61.0)	99.8	100.4
300	(91.4)	97.9	98.5
500	(152.4)	95.3	96.1
1000	(304.8)	91.7	92.6
2000	(609.6)	87.6	88.7
3000	(914.4)	84.9	86.2
5000	(1524)	81.1	82.7
10000	(3048)	74.9	77.1
20000	(6096)	67.3	69.8
30000	(9144)	62.2	64.6
50000	(15240)	55.2	56.9
Data Points		146	146

Table B2 (Cont'd)
b. Set and Run Information

Set	Model	Max Load	LT from SE	RT from SW	RT from NE	LT from NW
1.	OH-58		X	X	X	X
2.	OH-58			X		
27.	OH-58		X	X	X	X
28.	OH-58		X	X	X	X
4.	AH-1G		X	X	X	X
5.	AH-1G		X	X	X	X
39.	AH-1G		X	X	X	X
40.	AH-1G		X	X	X	X
6.	UH-1M		X	X	X	X
13.	UH-1M		X	X	X	X
29.	UH-1M		X	X	X	X
30.	UH-1M		X	X		X
15.	UH-1H		X	X	X	X
17.	UH-1H		X	X	X	X
25.	UH-1H		X	X	X	X
33.	UH-1H		X	X	X	X
16.	UH-1H	X	X	X	X	X
18.	UH-1H	X	X	X	X	X
26.	UH-1H	X	X	X	X	X
34.	UH-1H	X	X	X	X	X
19.	UH-1B		X	X	X	X
21.	UH-1B		X	X	X	X
23.	UH-1B		X	X	X	X
20.	UH-1B	X	X	X	X	X
22.	UH-1B	X	X	X	X	X
24.	UH-1B	X	X	X	X	X
8.	CH-47		X	X	X	X
14.	CH-47		X	X	X	X
37.	CH-47		X	X	X	X
7.	CH-47	X			X	
38.	CH-47	X	X	X	X	X
9.	CH-54		X	X	X	X
11.	CH-54		X	X	X	X
10.	CH-54	X				
12.	CH-54	X	X	X	X	X
31.	TH-55		X	X	X	X
32.	TH-55		X	X	X	X
35.	TH-55		X	X	X	X
36.	TH-55		X	X	X	X

Key: X = inside and outside turns

Table B3
Ascents and Descents Combined and Level Flyovers
a. SEL Values, dBA

Slant Distance ft	(m)	Ascents and Descents Combined	Level Flyovers
100	(30.5)	103.6	103.1
200	(61.0)	100.4	100.0
300	(91.4)	98.5	98.1
500	(152.4)	96.0	95.6
1000	(304.8)	92.5	92.0
2000	(609.6)	88.6	88.1
3000	(914.4)	86.0	85.6
5000	(1524)	82.5	82.0
10000	(3048)	76.8	76.3
20000	(6096)	69.6	69.1
30000	(9144)	64.4	64.1
50000	(15240)	56.8	56.6
Data Points		909	446

Table B3 (Cont'd)
b. Set and Run Information

Set	Model	Max Load	Level 360	Level 180	Ascent 360	Descent 180	Descent 360	Ascent 180
	Operation							
1.	OH-58		2	2	1	1	1	1
2.	OH-58		2	2	1		1	1
27.	OH-58		2	2	1	1	1	1
28.	OH-58		2	2	1	1	1	1
4.	AH-1G		2	2	1	1		1
5.	AH-1G		2	2	1	1	1	1
39.	AH-1G		2	2	1	1	1	1
40.	AH-1G		2	2	1	1	1	1
6.	UH-1M		2	2	1	1	1	1
13.	UH-1M		2	2	1	1	1	1
29.	UH-1M		2	2	1	1	1	1
30.	UH-1M		2	2	1	1	1	1
15.	UH-1H		2	2	1	1	1	1
17.	UH-1H		2	2	1	1	1	1
25.	UH-1H				1	1	1	1
33.	UH-1H		2	2	1	1	1	1
16.	UH-1H	X	2	2	1	1	1	1
18.	UH-1H	X	2	2	1	1	1	1
26.	UH-1H	X	2	2	1	1	1	1
34.	UH-1H	X	2	2	1	1	1	1
19.	UH-1B		2	2	1	1	1	1
21.	UH-1B		2	2	1	1	1	1
23.	UH-1B		2	2	1	1	1	1
20.	UH-1B	X	2	2	1	1	1	1
22.	UH-1B	X	2	2	1		1	1
24.	UH-1B	X	2	2	1	1	1	1
8.	CH-47		2	2	1	1	1	1
14.	CH-47		2	2	1	1	1	1
37.	CH-47		2	2	1	1	1	1
7.	CH-47	X	2	2	1	1	1	1
38.	CH-47	X	2	2	1	1	1	1
9.	CH-54		2	2	1	1	1	1
11.	CH-54		2	2	1	1	1	1
10.	CH-54	X		2	1	1	1	
12.	CH-54	X	2	2	1	1	1	1
31.	TH-55		2	2	1	1	1	1
32.	TH-55		2	2	1	1	1	1
35.	TH-55		2	2	1	1	1	1
36.	TH-55		2	2	1	1	1	1

Key: 1 = Ascents and descents (combined)
2 = Level flyovers

Table B4
UH-1H and CH-47 Aircraft Under Normal and Maximum Loading– Level Flyovers, Ascents and Descents (Combined)
a. SEL Values, dBA

Slant Distance ft	(m)	UH-1H Normal Loading	UH-1H Maximum Loading	CH-47 Normal Loading	CH-47 Maximum Loading
100	(30.5)	103.5	104.9	106.7	106.4
200	(61.0)	100.4	101.7	103.6	103.3
300	(91.4)	98.5	99.9	101.8	101.5
500	(152.4)	96.1	97.4	99.4	99.1
1000	(304.8)	92.6	94.0	96.1	95.8
2000	(609.6)	88.8	90.2	92.5	92.2
3000	(914.4)	86.3	87.7	90.2	89.9
5000	(1524)	82.7	84.1	86.9	86.7
10000	(3048)	77.0	78.4	81.7	81.6
20000	(6096)	69.8	71.1	74.9	74.9
30000	(9144)	64.8	66.1	69.9	70.0
50000	(15240)	57.6	58.9	62.2	62.5
Data Points		130	143	108	72

Table B4 (Cont'd)
b. Set and Run Information

		Operation						
		Max Load	Level 360	Level 180	Ascent 360	Descent 180	Descent 360	Ascent 180
Set	Model							
15.	UH-1H		1	1	1	1	1	1
17.	UH-1H		1	1	1	1	1	1
25.	UH-1H				1	1	1	1
33.	UH-1H		1	1	1	1	1	1
16.	UH-1H	X	2	2	2	2	2	2
18.	UH-1H	X	2	2	2	2	2	2
26.	UH-1H	X	2	2	2	2	2	2
34.	UH-1H	X	2	2	2	2	2	2
8.	CH-47		3	3	3	3	3	3
14.	CH-47		3	3	3	3	3	3
37.	CH-47		3	3	3	3	3	3
7.	CH-47	X	4	4	4	4	4	4
38.	CH-47	X	4	4	4	4	4	4

Key: 1 = UH-1H normal loading
2 = UH-1H maximum loading
3 = CH-47 normal loading
4 = CH-47 maximum loading

Table B5
UH-1B and CH-54 Aircraft Under Normal and Maximum Loading - Level Flyovers, Ascents and Descents (Combined)
a. SEL Values, dBA

Slant Distance ft	(m)	UH-1B Normal Loading	UH-1B Maximum Loading	CH-54 Normal Loading	CH-54 Maximum Loading
100	(30.5)	100.6	100.5	106.3	105.6
200	(61.0)	97.5	97.4	102.9	102.5
300	(91.4)	95.6	95.5	100.8	100.6
500	(152.4)	93.1	93.0	97.9	98.1
1000	(304.8)	89.6	89.5	93.8	94.4
2000	(609.6)	85.6	85.6	89.3	90.4
3000	(914.4)	83.0	83.1	86.4	87.7
5000	(1524)	79.3	79.4	82.3	83.9
10000	(3048)	73.3	73.5	75.9	77.8
20000	(6096)	65.6	65.9	68.1	70.2
30000	(9144)	60.0	60.3	62.6	64.8
50000	(15240)	51.7	52.0	54.6	56.8
Data Points		108	102	72	60

Table B5 (Cont'd)
b. Set and Run Information

		Operation						
		Mix Load	Level 360	Level 180	Ascent 360	Descent 180	Descent 360	Ascent 180
Set	Model							
19.	UH-1B		1	1	1	1	1	1
21.	UH-1B		1	1	1	1	1	1
23.	UH-1B		1	1	1	1	1	1
20.	UH-1B	X	2	2	2	2	2	2
22.	UH-1B	X	2	2	2	2	2	2
24.	UH-1B	X	2	2	2	2	2	2
9.	CH-54		3	3	3	3	3	3
11.	CH-54		3	3	3	3	3	3
10.	CH-54	X		4	4	4	4	
12.	CH-54	X	4	4	4	4	4	4

Key: 1 = UH-1B normal loading
2 = UH-1B maximum loading
3 = CH-54 normal loading
4 = CH-54 maximum loading

Table B6
All Aircraft, All Loadings–
Level Flyovers, Ascents and Descents (Combined)
a. SEL Values, dBA

Slant Distance ft	(m)	OH-58	AH-1G	UH-1M	UH-1H Normal and Maximum Loading
100	(30.5)	97.1	104.1	100.1	104.3
200	(61.0)	93.9	100.8	97.0	101.1
300	(91.4)	92.0	98.8	95.1	99.3
500	(152.4)	89.4	96.2	92.6	96.8
1000	(304.8)	85.7	92.5	89.1	93.4
2000	(609.6)	81.5	88.4	85.1	89.5
3000	(914.4)	78.8	85.6	82.4	87.1
5000	(1524)	74.8	81.7	78.7	83.5
10000	(3048)	68.4	75.1	72.7	77.8
20000	(6096)	60.1	66.9	65.2	70.6
30000	(9144)	54.1	61.1	60.0	65.5
50000	(15240)	45.1	52.8	52.3	58.3
Data Points		135	138	144	273

Slant Distance ft	(m)	UH-1B Normal and Maximum Loading	CH-47 Normal and Maximum Loading	CH-54 Normal and Maximum Loading	TH-55
100	(30.5)	100.6	106.6	106.0	98.7
200	(61.0)	97.4	103.5	102.7	95.4
300	(91.4)	95.5	101.6	100.7	93.4
500	(152.4)	93.1	99.3	98.0	90.7
1000	(304.8)	89.6	96.0	94.1	86.6
2000	(609.6)	85.6	92.4	89.8	81.8
3000	(914.4)	83.0	90.1	87.0	78.5
5000	(1524)	79.4	86.8	83.1	74.0
10000	(3048)	73.4	81.6	76.9	67.0
20000	(6096)	65.7	74.9	69.2	58.6
30000	(9144)	60.2	70.0	63.8	52.7
50000	(15240)	51.9	62.3	55.8	44.2
Data Points		210	180	132	143

Table B6 (Cont'd)
b. Set and Run Information

Set	Model	Max Load	Level 360	Level 180	Ascent 360	Descent 180	Descent 360	Ascent 180
1.	OH-58		1	1	1	1	1	1
2.	OH-58		1	1	1		1	1
27.	OH-58		1	1	1	1	1	1
28.	OH-58		1	1	1	1	1	1
4.	AH-1G		2	2	2	2		2
5.	AH-1G		2	2	2	2	2	2
39.	AH-1G		2	2	2	2	2	2
40.	AH-1G		2	2	2	2	2	2
6.	UH-1M		3	3	3	3	3	3
13.	UH-1M		3	3	3	3	3	3
29.	UH-1M		3	3	3	3	3	3
30.	UH-1M		3	3	3	3	3	3
15.	UH-1H		4	4	4	4	4	4
17.	UH-1H		4	4	4	4	4	4
25.	UH-1H				4	4	4	4
33.	UH-1H		4	4	4	4	4	4
16.	UH-1H	X	4	4	4	4	4	4
18.	UH-1H	X	4	4	4	4	4	4
26.	UH-1H	X	4	4	4	4	4	4
34.	UH-1H	X	4	4	4	4	4	4
19.	UH-1B		5	5	5	5	5	5
21.	UH-1B		5	5	5	5	5	5
23.	UH-1B		5	5	5	5	5	5
20.	UH-1B	X	5	5	5	5	5	5
22.	UH-1B	X	5	5	5		5	5
24.	UH-1B	X	5	5	5	5	5	5
8.	CH-47		6	6	6	6	6	6
14.	CH-47		6	6	6	6	6	6
37.	CH-47		6	6	6	6	6	6
7.	CH-47	X	6	6	6	6	6	6
38.	CH-47	X	6	6	6	6	6	6
9.	CH-54		7	7	7	7	7	7
11.	CH-54		7	7	7	7	7	7
10.	CH-54	X		7	7	7	7	
12.	CH-54	X	7	7	7	7	7	7
31.	TH-55		8	8	8	8	8	8
32.	TH-55		8	8	8	8	8	8
35.	TH-55		8	8	8	8	8	8
36.	TH-55		8	8	8	8	8	8

Key: 1 = OH-58
2 = AH-1G
3 = UH-1M
4 = UH-1H (normal and maximum loading)
5 = UH-1B (normal and maximum loading)
6 = CH-47 (normal and maximum loading)
7 = CH-54 (normal and maximum loading)
8 = TH-55

Table B7
Groups 1 Through 4 and All Aircraft–
Level Flyovers, Ascents and Descents (Combined)
a. SEL Values, dBA

Slant Distance ft	(m)	Group 1 CH-47*	Group 2 AH-1G, UH-1H* CH-54*	Group 3 UH-1M, UH-1B*	Group 4 OH-58, TH-55	All Aircraft
100	(30.5)	106.6	104.7	100.4	98.0	103.4
200	(61.0)	103.5	101.5	97.3	94.8	100.3
300	(91.4)	101.6	99.5	95.4	92.8	98.4
500	(152.4)	99.3	97.0	92.9	90.1	95.9
1000	(304.8)	96.0	93.4	89.4	86.2	92.3
2000	(609.6)	92.4	89.4	85.4	81.7	88.4
3000	(914.4)	90.1	86.7	82.8	78.6	85.9
5000	(1524)	86.8	83.0	79.1	74.4	82.3
10000	(3048)	81.6	77.0	73.1	67.7	76.6
20000	(6096)	74.9	69.5	65.5	59.4	69.4
30000	(9144)	70.0	64.3	60.1	53.4	64.3
50000	(15240)	62.3	56.8	52.0	44.6	56.7
Data Points		180	543	354	278	1355

*Normal and maximum loading.

Table B7 (Cont'd)
b. Set and Run Information

Set	Model	Max Load	Level 360	Level 180	Ascent 360	Descent 180	Descent 360	Ascent 180
	Operation							
Set	**Model**							
1.	OH-58		4	4	4	4	4	4
2.	OH-58		4	4	4		4	4
27.	OH-58		4	4	4	4	4	4
28.	OH-58		4	4	4	4	4	4
4.	AH-1G		2	2	2	2		2
5.	AH-1G		2	2	2	2	2	2
39.	AH-1G		2	2	2	2	2	2
40.	AH-1G		2	2	2	2	2	2
6.	UH-1M		3	3	3	3	3	3
13.	UH-1M		3	3	3	3	3	3
29.	UH-1M		3	3	3	3	3	3
30.	UH-1M		3	3	3	3	3	3
15.	UH-1H		2	2	2	2	2	2
17.	UH-1H		2	2	2	2	2	2
25.	UH-1H				2	2	2	2
33.	UH-1H		2	2	2	2	2	2
16.	UH-1H	X	2	2	2	2	2	2
18.	UH-1H	X	2	2	2	2	2	2
26.	UH-1H	X	2	2	2	2	2	2
34.	UH-1H	X	2	2	2	2	2	2
19.	UH-1B		3	3	3	3	3	3
21.	UH-1B		3	3	3	3	3	3
23.	UH-1B		3	3	3	3	3	3
20.	UH-1B	X	3	3	3	3	3	3
22.	UH-1B	X	3	3	3		3	3
24.	UH-1B	X	3	3	3	3	3	3
8.	CH-47		1	1	1	1	1	1
14.	CH-47		1	1	1	1	1	1
37.	CH-47		1	1	1	1	1	1
7.	CH-47	X	1	1	1	1	1	1
38.	CH-47	X	1	1	1	1	1	1
9.	CH-47		2	2	2	2	2	2
11.	CH-54		2	2	2	2	2	2
10.	CH-54	X		2	2	2	2	2
12.	CH-54	X	2	2	2	2	2	2
31.	TH-55		4	4	4	4	4	4
32.	TH-55		4	4	4	4	4	4
35.	TH-55		4	4	4	4	4	4
36.	TH-55		4	4	4	4	4	4

Key: 1 = Group 1 (CH-47 normal and maximum loading)
2 = Group 2 (AH-1G, UH-1H normal and maximum loading, and CH-54 normal and maximum loading)
3 = Group 3 (UH-1M, UH-1B normal and maximum loading)
4 = Group 4 (OH-58 and TH-55)

Table B8
Wind Direction Effects for All Aircraft (Normal and Maximum Loading)– Level Flyovers, Ascents and Descents (Combined)
a. SEL Values, dBA

Slant Distance ft	(m)	Head Wind	Tail Wind	Port Wind	Starboard Wind
100	(30.5)	101.4	101.6	104.4	104.0
200	(61.0)	98.2	98.5	101.1	100.9
300	(91.4)	96.3	96.6	99.1	99.0
500	(152.4)	93.9	94.1	96.6	96.6
1000	(304.8)	90.3	90.6	93.0	93.2
2000	(609.6)	86.4	86.7	89.0	89.3
3000	(914.4)	83.8	84.1	86.5	86.8
5000	(1524)	80.3	80.6	82.8	83.3
10000	(3048)	74.8	74.9	76.9	77.7
20000	(6096)	68.0	67.8	69.5	70.4
30000	(9144)	63.1	62.6	64.3	65.1
50000	(15240)	56.0	54.7	56.6	57.1
Data Points		137	107	114	113

Table B8 (Cont'd)
b. Set and Run Information

Set	Model	Max Load	Level 360	Level 180	Ascent 360	Descent 180	Descent 360	Ascent 180
1.	OH-58		2	1	2	1	2	1
2.	OH-58		2	1	2		2	1
28.	OH-58			2		2		
5.	AH-1G		3	4	3	4	3	4
6.	UH-1M		3	4	3	4	3	4
29.	UH-1M		3					
30.	UH-1M				1			
17.	UH-1H				3	4		
25.	UH-1H				1		3	
33.	UH-1H	X	4				4	
16.	UH-1H	X			1	2		
18.	UH-1H	X		2				
26.	UH-1H	X	3	4				1
23.	UH-1B		4	3				
24.	UH-1B	X	4					
14.	CH-47		3	4	3	4	3	4
37.	CH-47		2	1		1	2	1
11.	CH-54			3	4			1
10.	CH-54	X					4	
12.	CH-54	X		3	4			
31.	TH-55		2	1	2	1	2	1
32.	TH-55		2	1	2	1	2	1
35.	TH-55		4	3		3	1	3
36.	TH-55		1		1			

Key: 1 = Head wind
2 = Tail wind
3 = Port wind
4 = Starboard wind

Table B9
Effects of Head and Tail Winds and Port and Starboard Winds for All Aircraft (Normal and Maximum Loadings)– Level Flyovers, Ascents and Descents (Combined)
a. SEL Values, dBA

Slant Distance ft	(m)	Head and Tail Winds (Combined)	Port and Starboard Winds (Combined)
100	(30.5)	101.4	104.4
200	(61.0)	98.2	101.1
300	(91.4)	96.3	99.1
500	(152.4)	93.9	96.6
1000	(304.8)	90.3	93.0
2000	(609.6)	86.4	89.0
3000	(914.4)	83.8	86.5
5000	(1524)	80.3	82.8
10000	(3048)	74.8	76.9
20000	(6096)	68.0	69.5
30000	(9144)	63.1	64.3
50000	(15240)	56.0	56.6
Data Points		137	114

Table B9 (Cont'd)
b. Set and Run Information

Set	Model	Max Load	Level 360	Level 180	Ascent 360	Descent 18G	Descent 360	Ascent 180
1.	OH-58			2		2		2
2.	OH-58			2				2
5.	AH-1G		1		1		1	
6.	UH-1M		1		1		1	
29.	UH-1M		1					
30.	UH-1M				2			
17.	UH-1H				1			
25.	UH-1H				2	1		
16.	UH-1H	X			2			
26.	UH-1H	X		1				2
23.	UH-1B			1				
20.	UH-1B	X	2					
14.	CH-47		1		1		1	
37.	CH-47			2		2		2
11.	CH-54			1				2
12.	CH-54	X		1				
31.	TH-55			2		2		2
32.	TH-55			2		2		2
35.	TH-55			1		1	2	1
36.	TH-55				2			

Key: 1 = Head and tail winds combined
2 = Port and starboard winds combined

Table B10
Effects of Wind Velocity for All Aircraft (Normal and Maximum Loading)–
Level Flyovers, Ascents and Descents (Combined)
a. SEL Values, dBA

Slant Distance ft	(m)	0 to 5 knots (0 to 154 m/sec)	5 to 10 knots (154 to 309 m/sec)	10 to 15 knots (309 to 463 m/sec)	15 to 20 knots (463 to 617 m/sec)
100	(30.5)	103.8	102.2	103.2	101.7
200	(61.0)	100.6	100.1	100.0	98.5
300	(91.4)	98.7	98.2	98.0	96.6
500	(152.4)	96.2	95.7	95.5	94.2
1000	(304.8)	92.6	92.2	91.9	90.6
2000	(609.6)	88.7	88.4	87.9	86.6
3000	(914.4)	86.2	85.9	85.3	84.0
5000	(1524)	82.7	82.3	81.7	80.2
10000	(3048)	77.1	76.6	75.8	74.0
20000	(6096)	70.0	69.5	68.3	66.0
30000	(9144)	64.9	64.4	63.0	60.5
50000	(15240)	57.4	56.8	55.1	52.4
Data Points		578	472	275	30

Table B10 (Cont'd)
b. Set and Run Information

Set	Model	Operation: Max Load	Level 360	Level 180	Ascent 360	Descent 180	Descent 360	Ascent 180
1.	OH-58		3	2	3	3	2	3
2.	OH-58		4	3	3		3	2
27.	OH-58		1	1	1	1	1	1
28.	OH-58		2	2	1	1	1	1
4.	AH-1G		3	3	4	3		4
5.	AH-1G		3	3	3	4	3	3
39.	AH-1G		1	1	1	1	1	1
40.	AH-1G		1	1	1	1	1	1
6.	UH-1M		3	3	3	3	3	3
13.	UH-1M			2	2			
29.	UH-1M		1	2	2	1	1	2
30.	UH-1M		1	1	1	1	2	1
15.	UH-1H		1	2	2	2	2	2
17.	UH-1H		1	1	2	1	1	1
25.	UH-1H				1	1	1	1
33.	UH-1H		2	2	2	2	2	1
16.	UH-1H	X	1	2	2	1	1	1
18.	UH-1H	X	1	1	1	1	1	2
26.	UH-1H	X	1	1	1	1	1	1
34.	UH-1H	X	2	2	2	2	2	2
19.	UH-1B		1	2	2	2	2	2
21.	UH-1B		2	2	2	2	1	2
23.	UH-1B		1	1	1	1	1	1
20.	UH-1B	X	1	1	1	2	2	2
22.	UH-1B	X	3	2	2		2	2
24.	UH-1B	X	1	1	1	1	1	1
8.	CH-47		1	1	1	1	1	1
14.	CH-47		2	2	2	2	2	2
37.	CH-47		1	1	1	1	2	2
7.	CH-47	X	3	3	3	2	3	4
38.	CH-47	X	1	1	1	1	1	1
9.	CH-54		1	1	1	1	1	1
11.	CH-54		3	2	2	2	3	3
10.	CH-54	X		2	2	2	2	
12.	CH-54	X	2	3	3	3	2	3
31.	TH-55		2	3	2	2	2	2
32.	TH-55		3	3	3	3	2	3
35.	TH-55		3	2	1	3	2	2
36.	TH-55		1	2	2	2	2	3

Key: 1 = 0 to 5 knots (0 to 154 m/sec)
2 = 5 to 10 knots (154 to 309 m/sec)
3 = 10 to 15 knots (309 to 463 m/sec)
4 = 15 to 20 knots (463 to 617 m/sec)

Table B11
Effects of Sideline and Beneath Microphones for All Aircraft (Normal and Maximum Loading)– Level Flyovers, Ascents and Descents (Combined)
a. SEL Values, dBA

Slant Distance ft	(m)	Sideline	Beneath	Sideline and Beneath (Combined)
100	(30.5)	102.8	103.3	103.0
200	(61.0)	99.5	100.2	99.8
300	(91.4)	97.5	98.3	97.8
500	(152.4)	95.0	95.9	95.3
1000	(304.8)	91.3	92.4	91.7
2000	(609.6)	87.3	88.6	97.8
3000	(914.4)	84.7	86.1	85.2
5000	(1524)	81.0	82.7	81.6
10000	(3048)	75.0	77.2	75.9
20000	(6096)	67.6	70.3	68.7
30000	(9144)	62.5	65.4	63.7
50000	(15240)	55.0	58.1	56.3
Data Points		167	84	251

Table B11 (Cont'd)
b. Set and Run Information

Set	Model	Max Load	Level 360	Level 180	Ascent 360	Descent 180	Descent 360	Ascent 180
1.	OH-58			X		X		X
2.	OH-58			X				X
5.	AH-1G		X		X		X	
6.	UH-1M		X		X		X	
29.	UH-1M		X					
30.	UH-1M			1	X			
17.	UH-1H				X			
25.	UH-1H				X		X	
16.	UH-1H	X			X			
26.	UH-1H	X	X					X
23.	UH-1B			X				
20.	UH-1B	X	X					
14.	CH-47		X		X		X	
37.	CH-47			X		X		X
11.	CH-54			X				X
12.	CH-54	X		X				
31.	TH-55			X		X		X
32.	TH-55			X		X		X
35.	TH-55			X		X		X
36.	TH-55		X		X			

Key: X = Sideline and beneath microphones both represented
1 = Sideline microphones

Table B12
Landing Microphones and Level Flyovers—All Aircraft
(Normal and Maximum Loading)
a. SEL Values, dBA

Slant Distance ft	(m)	Microphones 3 and 5	Microphones 2 and 6	Microphone 1	Level Flyover
100	(30.5)	107.3	112.1	105.9	103.1
200	(61.0)	104.0	108.6	102.6	100.0
300	(91.4)	102.0	106.4	100.6	98.1
500	(152.4)	99.4	103.5	98.0	95.6
1000	(304.8)	95.6	99.2	94.2	92.0
2000	(609.6)	91.4	94.7	90.2	88.1
3000	(914.4)	88.7	91.8	87.6	85.6
5000	(1524)	85.0	87.8	83.9	82.0
10000	(3048)	79.0	81.3	78.1	76.3
20000	(6096)	71.6	73.5	70.6	69.1
30000	(9144)	66.4	68.3	65.2	64.1
50000	(15240)	58.6	60.9	56.9	56.6
Data Points		74	74	57	446

Table B12 (Cont'd)
b. Set and Run Information

Set	Model	Operation: Max Load	Level 360	Level 180	Landing
1.	OH-58		4	4	123
2.	OH-58		4	4	123
27.	OH-58		4	4	123
28.	OH-58		4	4	123
4.	AH-1G		4	4	123
5.	AH-1G		4	4	123
39.	AH-1G		4	4	123
40.	AH-1G		4	4	123
6.	UH-1M		4	4	
13.	UH-1M		4	4	123
29.	UH-1M		4	4	123
30.	UH-1M		4	4	123
15.	UH-1H		4	4	123
17.	UH-1H		4	4	123
25.	UH-1H				123
33.	UH-1H		4	4	123
16.	UH-1H	X	4	4	123
18.	UH-1H	X	4	4	123
26.	UH-1H	X	4	4	123
34.	UH-1H	X	4	4	123
19.	UH-1B		4	4	123
21.	UH-1B		4	4	123
23.	UH-1B		4	4	123
20.	UH-1B	X	4	4	123
22.	UH-1B	X	4	4	123
24.	UH-1B	X	4	4	123
8.	CH-47		4	4	123
14.	CH-47		4	4	123
37.	CH-47		4	4	123
7.	CH-47	X	4	4	123
38.	CH-47	X	4	4	123
9.	CH-54		4	4	123
11.	CH-54		4	4	123
10.	CH-54	X		4	
12.	CH-54	X	4	4	123
31.	TH-55		4	4	123
32.	TH-55		4	4	123
35.	TH-55		4	4	123
36.	TH-55		4	4	123

Key: 1 = Microphones 3 and 5
2 = Microphones 2 and 6
3 = Microphone 1
4 = Level flyovers

Table B13
Landings and Level Flyovers--All Aircraft
(Normal and Maximum Loading)
a. SEL Values, dBA

Slant Distance ft	(m)	Landings	Level Flyovers
100	(30.5)	109.8	103.1
200	(61.0)	106.3	100.0
300	(91.4)	104.2	98.1
500	(152.4)	101.4	95.6
1000	(304.8)	97.3	92.0
2000	(609.6)	93.1	88.1
3000	(914.4)	90.4	85.6
5000	(1524)	86.6	82.0
10000	(3048)	80.5	76.3
20000	(6096)	73.1	69.1
30000	(9144)	67.9	64.1
50000	(15240)	60.2	56.6
Data Points		222	446

Table B13 (Cont'd)
Standard Run Information

Set	Model	Operation: Max Load	Level 360	Level 180	Landing
1.	OH-58		2	2	1
2.	OH-58		2	2	1
27.	OH-58		2	2	1
28.	OH-58		2	2	1
4.	AH-1G		2	2	1
5.	AH-1G		2	2	1
39.	AH-1G		2	2	1
40.	AH-1G		2	2	1
6.	UH-1M		2	2	
13.	UH-1M		2	2	1
29.	UH-1M		2	2	1
30.	UH-1M		2	2	1
15.	UH-1H		2	2	1
17.	UH-1H		2	2	1
25.	UH-1H				1
33.	UH-1H		2	2	1
16.	UH-1H	X	2	2	1
18.	UH-1H	X	2	2	1
26.	UH-1H	X	2	2	1
34.	UH-1H	X	2	2	1
19.	UH-1B		2	2	1
21.	UH-1B		2	2	1
23.	UH-1B		2	2	1
20.	UH-1B	X	2	2	1
22.	UH-1B	X	2	2	1
24.	UH-1B	X	2	2	1
8.	CH-47		2	2	1
14.	CH-47		2	2	1
37.	CH-47		2	2	1
7.	CH-47	X	2	2	1
38.	CH-47	X	2	2	1
9.	CH-54		2	2	1
11.	CH-54		2	2	1
10.	CH-54	X		2	
12.	CH-54	X	2	2	1
31.	TH-55		2	2	1
32.	TH-55		2	2	1
35.	TH-55		2	2	1
36.	TH-55		2	2	1

Key: 1 = Landings
2 = Level flyovers

Table B14
Takeoff Microphones and Level Flyovers – All Aircraft (Normal and Maximum Loading)
a. SEL Values, dBA

Slant Distance ft	(m)	Microphone 4	Microphones 3 and 5	Level Flyover
100	(30.5)	113.4	102.6	103.1
200	(61.0)	110.1	99.4	100.0
300	(91.4)	108.2	97.4	98.1
500	(152.4)	105.6	94.9	95.6
1000	(304.8)	101.9	91.1	92.0
2000	(609.6)	98.0	87.0	88.1
3000	(914.4)	95.4	84.3	85.6
5000	(1524)	91.8	80.5	82.0
10000	(3048)	86.1	74.4	76.3
20000	(6096)	78.9	66.7	69.1
30000	(9144)	73.7	61.4	64.1
50000	(15240)	65.8	53.6	56.6
Data Points		37	74	446

Table B14 (Cont'd)
b. Set and Run Information

		Operation			
		Max Load	Level 360	Level 180	Takeoff
Set	Model				
1.	OH-58		3	3	12
2.	OH-58		3	3	12
27.	OH-58		3	3	12
28.	OH-58		3	3	12
4.	AH-1G		3	3	12
5.	AH-1G		3	3	12
39.	AH-1G		3	3	12
40.	AH-1G		3	3	12
6.	UH-1M		3	3	
13.	UH-1M		3	3	12
29.	UH-1M		3	3	12
30.	UH-1M		3	3	12
15.	UH-1H		3	3	12
17.	UH-1H		3	3	12
25.	UH-1H				12
33.	UH-1H		3	3	12
16.	UH-1H	X	3	3	12
18.	UH-1H	X	3	3	12
26.	UH-1H	X	3	3	12
34.	UH-1H	X	3	3	12
19.	UH-1B		3	3	12
21.	UH-1B		3	3	12
23.	UH-1B		3	3	12
20.	UH-1B	X	3	3	12
22.	UH-1B	X	3	3	12
24.	UH-1B	X	3	3	12
8.	CH-47		3	3	12
14.	CH-47		3	3	12
37.	CH-47		3	3	12
7.	CH-47	X	3	3	12
38.	CH-47	X	3	3	12
9.	CH-54		3	3	12
11.	CH-54		3	3	12
10.	CH-54	X		3	
12.	CH-54	X	3	3	12
31.	TH-55		3	3	12
32.	TH-55		3	3	12
35.	TH-55		3	3	12
36.	TH-55		3	3	12

Key: 1 = Microphone 4
2 = Microphones 3 and 5
3 = Level flyovers

APPENDIX C:

L_{eq} PLOTS FOR STATIC OPERATIONS

This appendix provides directivity patterns by aircraft model for in-ground (solid lines) and out-of-ground (dashed lines) effect hovers (Figures C1 through C8). Helicopters were piloted to face the wind at all times and the arrow at the top of each polar plot represents the nose (0 degrees). At the lower portion of each figure, A-weighted L_{eq} values are presented in clockwise order for in-ground (IG) and out-of-ground (OG) effect hovers beginning at 0 degrees.

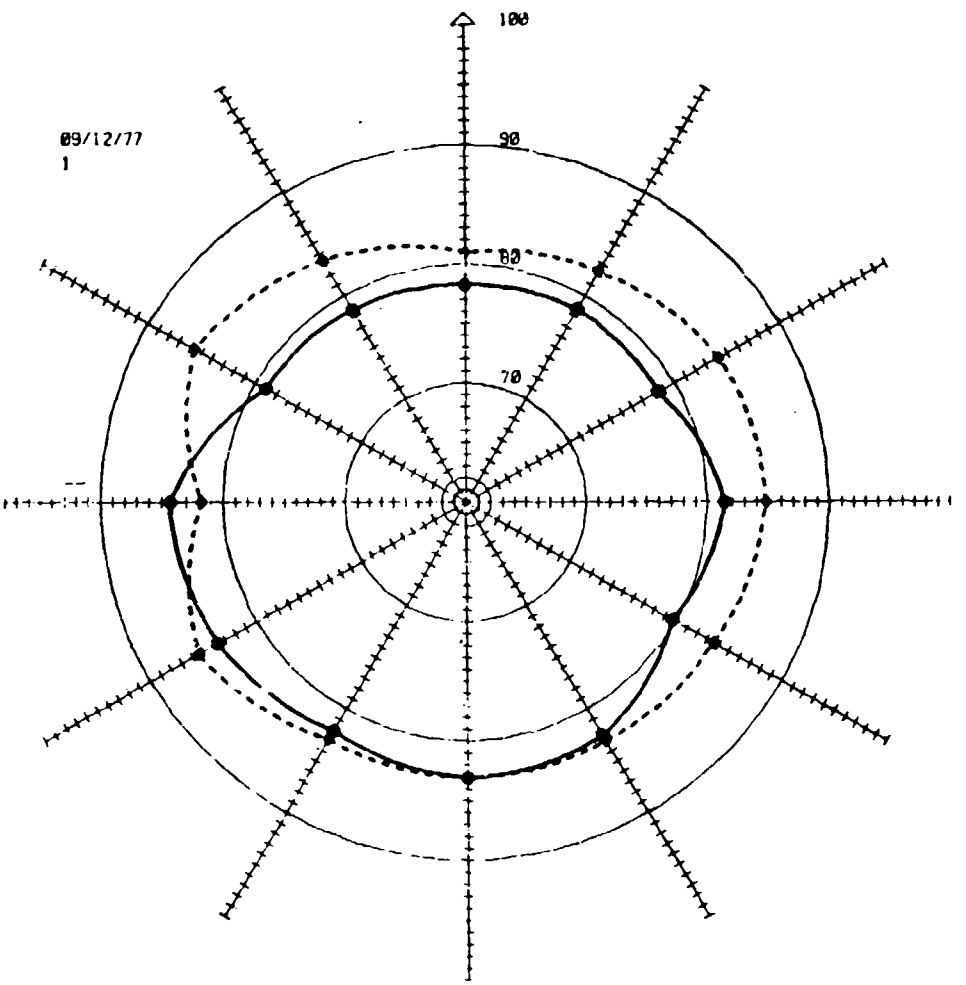

SETS:	1											27
IG:	78.2	78.6	78.5	81.4	79.7	82.6	83.1	82.1	83.6	84.3	79.0	78.6
OG:	81.0	82.3	84.2	84.8	83.6	83.1	83.0	82.9	85.5	81.7	85.7	83.4

Figure C1. Directivity pattern for OH-58.

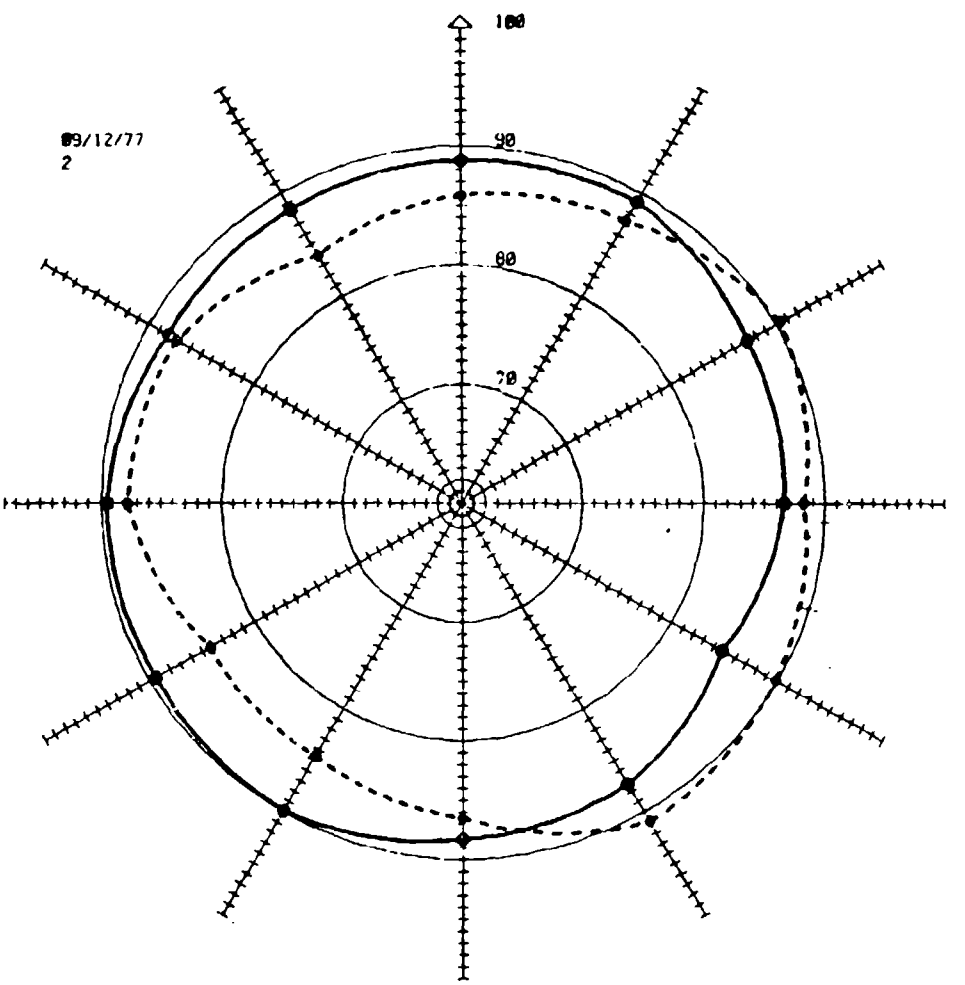

SETS:	4	5	39									
IG:	88.8	89.2	87.2	86.6	84.8	87.3	88.3	89.9	89.4	89.5	88.1	88.4
OG:	85.8	87.3	90.4	88.2	89.8	91.0	86.5	84.6	84.3	87.7	87.3	83.9

Figure C2. Directivity pattern for AH-1G.

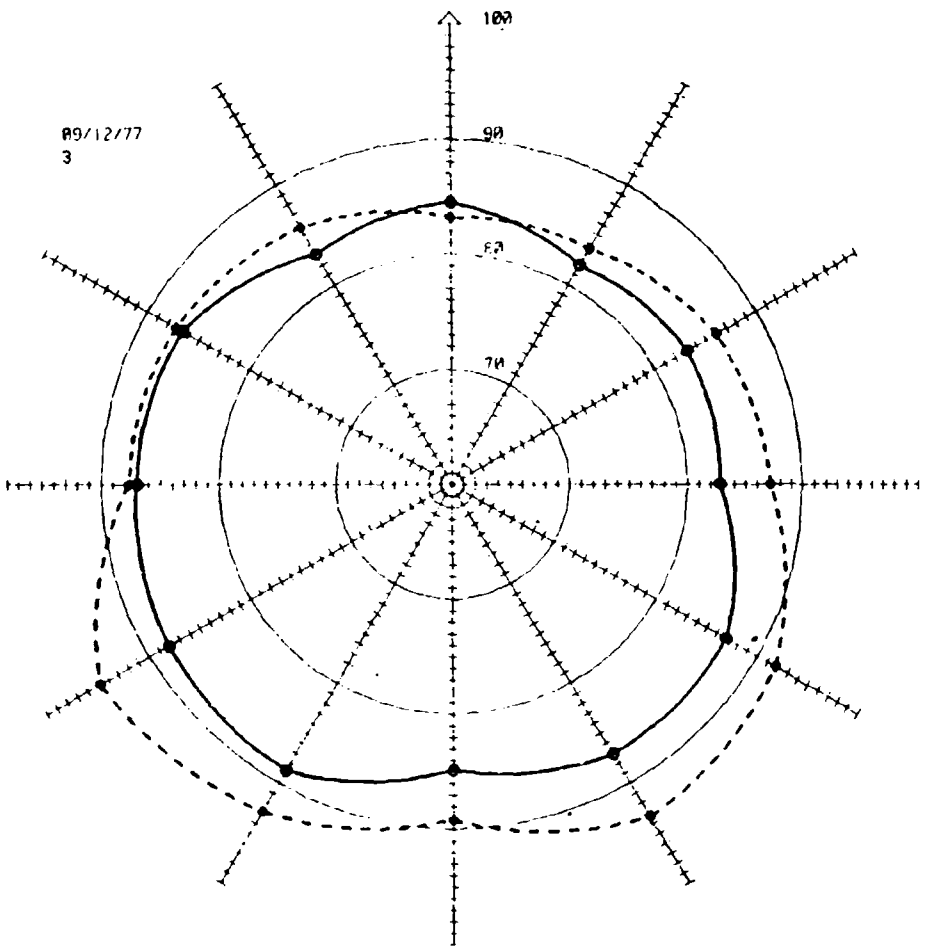

SLTS	19	20	21	22	23	24						
IG	84.5	81.9	83.1	82.8	86.9	87.1	84.8	88.7	88.1	87.0	86.6	83.1
OG	83.2	83.6	86.0	87.2	91.8	93.4	89.2	92.9	94.8	87.6	87.2	85.7

Figure C3. Directivity pattern for UH-1B.

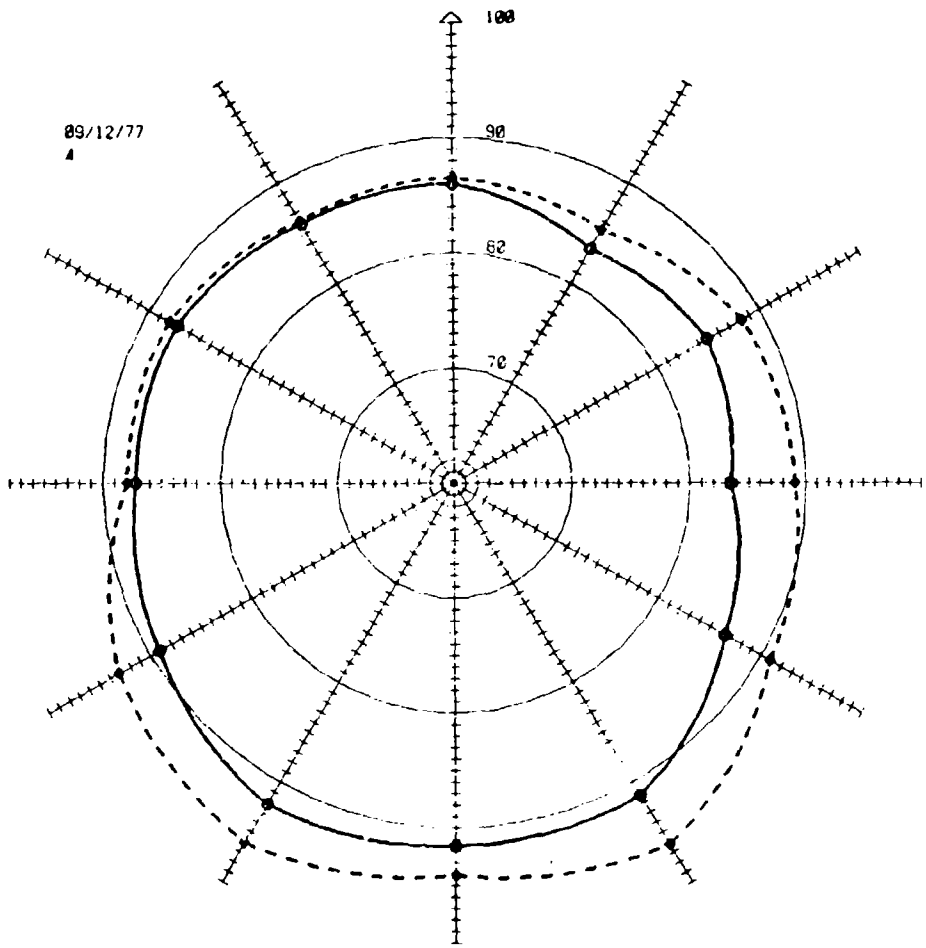

SI-TS:	15	16	17	18	25	26	33						
IG:	86.0	83.4	84.9	83.4	86.4	91.3	91.5	92.2	89.1	87.2	87.3	85.9
OG:	86.5	85.3	88.2	89.0	90.9	96.3	94.1	96.1	93.1	87.9	88.0	86.2

Figure C4. Directivity pattern for UH-1H (normal and maximum loading).

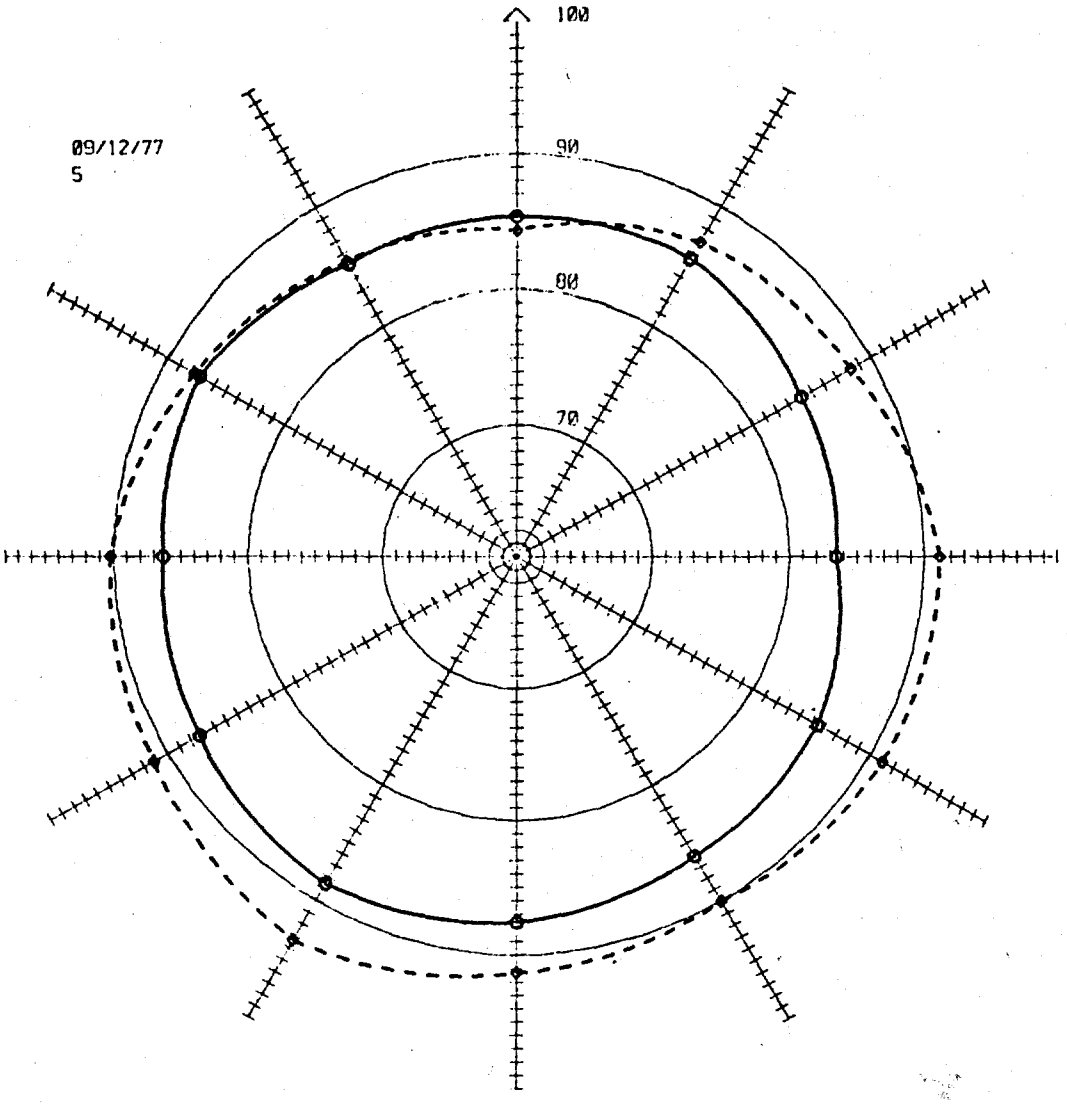

SETS:	6	13	29	30	3							
IG:	85.3	85.5	84.1	83.4	85.5	86.1	87.6	88.6	87.3	86.3	87.3	85.1
OG:	84.3	86.9	88.3	91.1	91.1	90.0	91.3	93.4	91.2	90.2	87.7	85.4

Figure C5. Directivity pattern for UH-1M (normal and maximum loading).

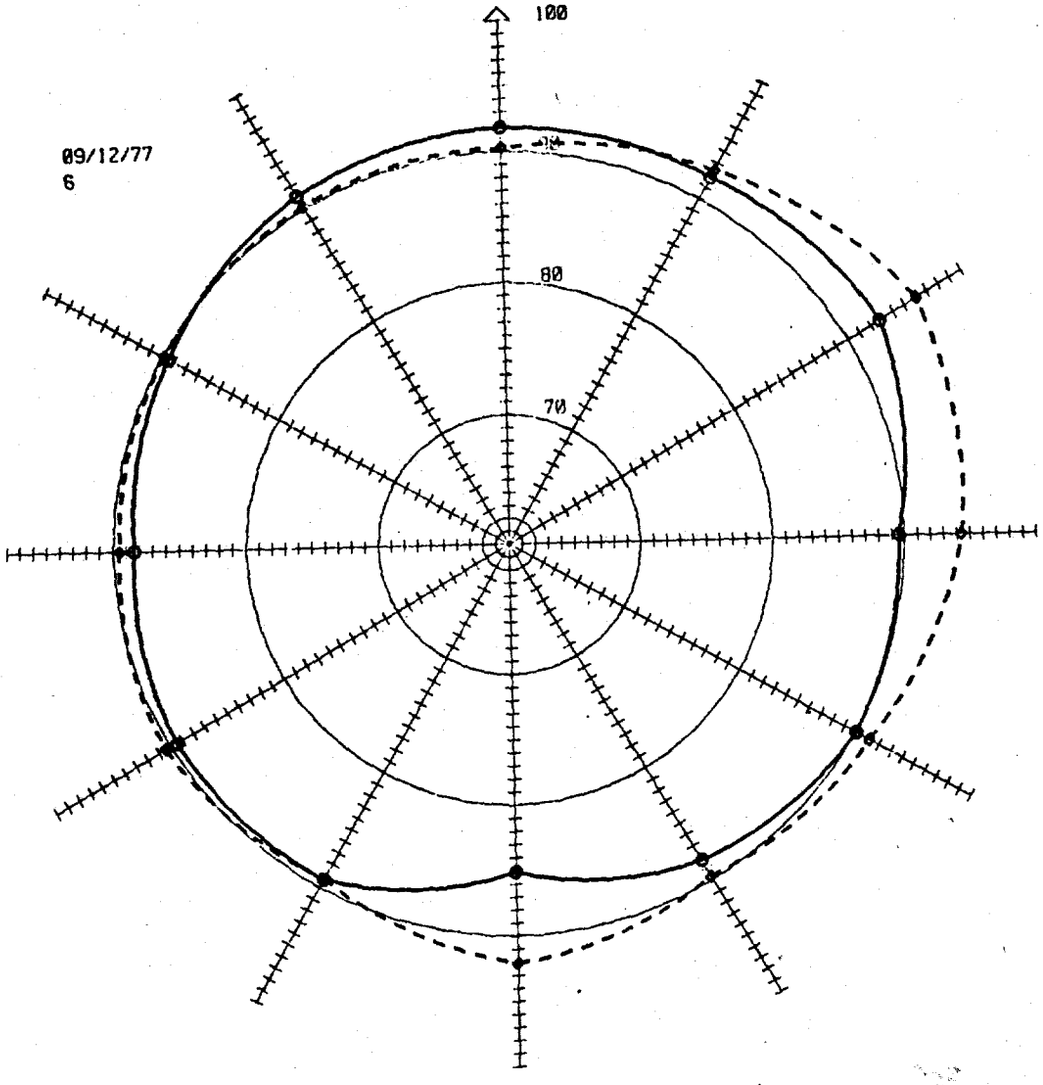

SETS:	7	8	14	37	38							
IG:	91.8		91.8	92.8	89.5	90.0	88.3	85.1	89.3	89.5	88.4	89.5	91.1
OG:	90.2		92.4	96.0	94.4	91.2	89.7	92.1	89.3	90.4	89.5	89.9	90.2

Figure C6. Directivity pattern for CH-47 (normal and maximum loading).

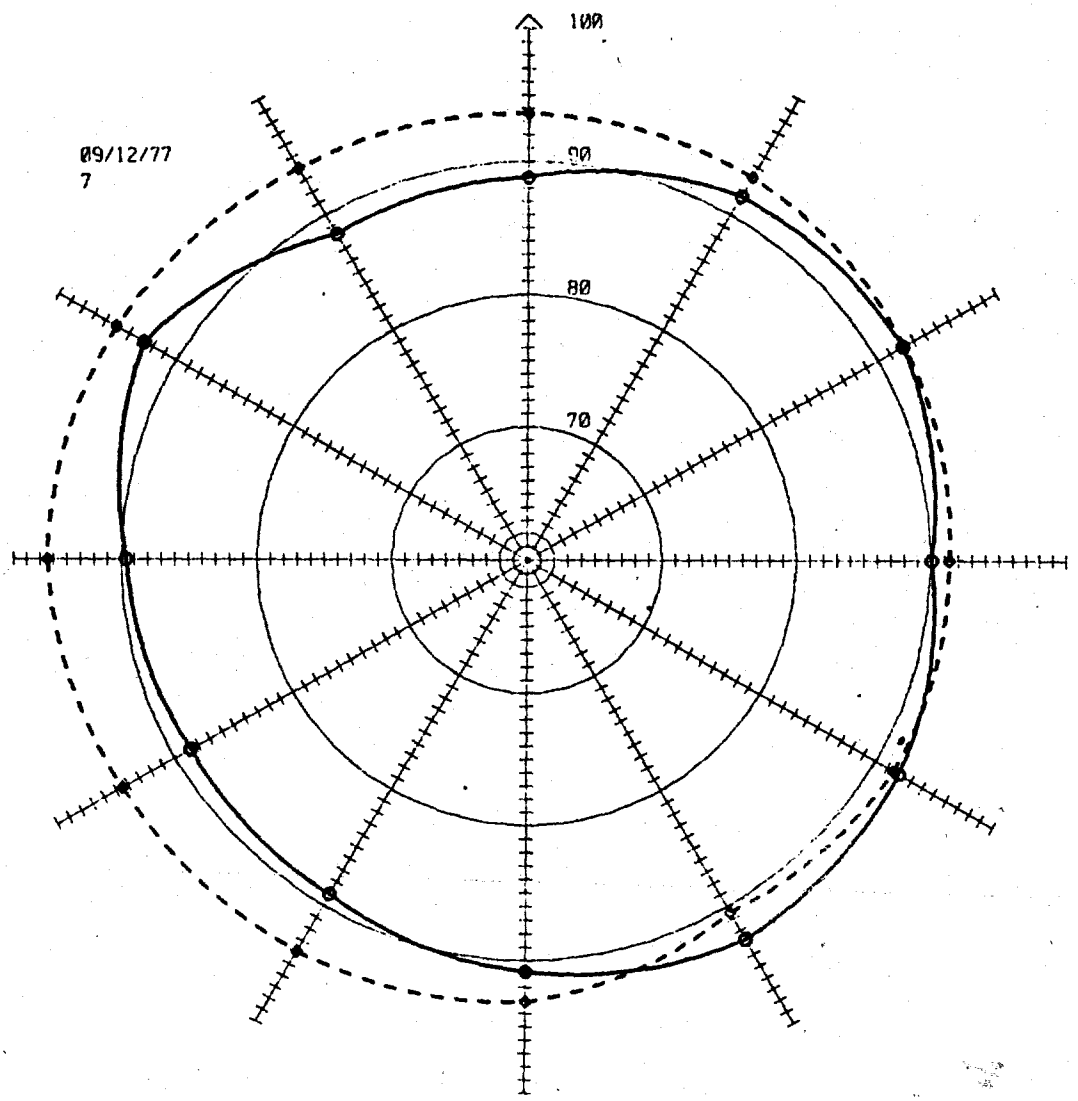

SETS:	9	11	12									
IG:	88.8	91.6	92.1	90.1	92.0	92.8	90.8	89.1	88.6	89.6	92.7	88.3
OG:	93.6	93.2	92.2	91.3	91.5	90.5	93.1	93.9	94.5	95.5	95.1	94.0

Figure C7. Directivity pattern for CH-54 (normal and maximum loading).

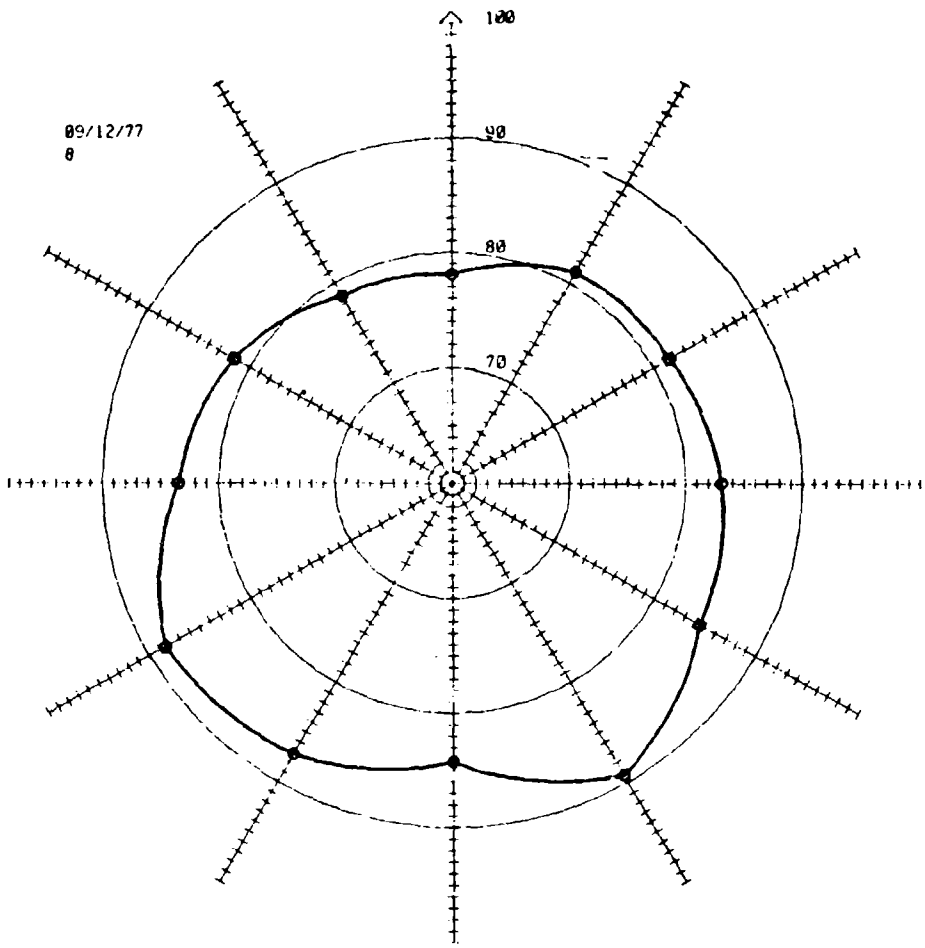

SETS:	31	32	35	36								
IG:	78.1	81.1	81.5	83.0	84.5	89.3	84.3	87.2	88.4	83.5	81.5	78.7

Figure C8. Directivity pattern for TH-55.

CERL DISTRIBUTION

P[illegible] Arsenal
[illegible] SMUPA-VP3

US Army, Europe
ATTN: AEAEN

Director of Facilities Engr
APO New York 09827

HQ US Army Materiel
DARCOM
ATTN: DRCPA-E/E. Proudman
ATTN: J. Pace
501 Eisenhower Ave
Alexandria, VA 22333

DARCOM STIT-EUR
APO New York 09710

HQDA (SGRD-EDE)

Chief of Engineers
ATTN: DAEN-MCC-E/D. Spivey
ATTN: DAEN-ASI-L (2)
ATTN: DAEN-FEB
ATTN: DAEN-FEP
ATTN: DAEN-FEZ-A
ATTN: DAEN-MCZ-S
ATTN: DAEN-RDL
ATTN: DAEN-MCE-A/W. B. Holmes
ATTN: DAEN-MCC-E/P. Van Parys
ATTN: DAEN-MCE-P/F. P. Beck (2)
ATTN: DAEN-MCE-P/J. Halligan
ATTN: DAEN-ZCE-D/D. M. Benton (2)
ATTN: DAEN-ZCE
ATTN: DAEN-PMS (7)
for forwarding to:
National Defense HQDA
Director General of Construction
Ottawa, Ontario K1AOK2
Canada

Canadian Forces Liaison Officer (4)
U.S. Army Mobility Equipment
Research and Development Command
Ft Belvoir, VA 22060

Div of Bldg Research
National Research Council
Montreal Road
Ottawa, Ontario K1AOR6
Canada

Airports and Const. Services Dir.
Technical Information Reference
Centre
KAOL, Transport Canada Building
Place de Ville
Ottawa, Ontario K1AON8
Canada

Ft Belvoir, VA 22060
ATTN: Kingman Bldg, Library

DFAE Envir Quality Section
ATTN: Mike Halla
Ft Carson, CO 80192

US Training and Doctrine Command
ATTN: ATEN-FE-E/D. Dery
ATTN: James L. Aikin, Jr.,
ATTN: Chief, Envr Branch
ATTN: ATEN
Ft Monroe, VA 23651

Ft McPherson, GA 30330
ATTN: AFEN-FEB
ATTN: Robert Montgomery
ATTN: Robert Jarrett

US Army Medical Bioengineering
R&D Laboratory
Envr Protection Res Div
ATTN: LTC LeRoy H. Reuter
Ft Detrick
Frederick, MD 21701

US Army Aeromedical Research Lab
ATTN: Robert T. Camp, Jr.
ATTN: CPT J. Patterson
Box 577
Ft Rucker, AL 36360

USA-WES
ATTN: Library
ATTN: Jack [illegible]/WESSE

6th US Army
ATTN: AFKC-EN

US Army Engineer District
New York
ATTN: Chief, Design Br
Philadelphia
ATTN: Library
ATTN: Chief, NAPEN-E
Baltimore
ATTN: Chief, Engr Div
Norfolk
ATTN: Chief, NAOEN-D
Huntington
ATTN: Chief, ORHED
Wilmington
ATTN: Chief, SWAEN-D
Savannah
ATTN: Library
ATTN: Chief, SASAS-L
Mobile
ATTN: Chief, SAMEN-D
Memphis
ATTN: Library
Louisville
ATTN: Chief, Engr Div
Detroit
ATTN: Library
St. Paul
ATTN: Chief, ED-D
Rock Island
ATTN: Library
ATTN: Chief, Engr Div
St Louis
ATTN: Library
ATTN: Chief, ED-D
Kansas City
ATTN: Library (2)
Omaha
ATTN: Chief, Engr Div
New Orleans
ATTN: Library
ATTN: Chief, LMNED-DG
Little Rock
ATTN: Chief, Engr Div
Tulsa
ATTN: Chief, Engr Div
ATTN: Library
Fort Worth
ATTN: Library
ATTN: Chief, SWFED-D
ATTN: Bill G. Daniels
ATTN: Royce W. Mullens, Water
Resource Planning
Albuquerque
ATTN: Library
San Francisco
ATTN: Chief, Engr Div
Sacramento
ATTN: Chief, SPKED-D
Far East
ATTN: Chief, Engr Div
Japan
ATTN: Library
Portland
ATTN: Library
Seattle
ATTN: Chief, EN-DB-ST
Walla Walla
ATTN: Library
ATTN: Chief, Engr Div
Alaska
ATTN: Library
ATTN: NPADE-R

US Army Engineer Division
Europe
ATTN: Technical Library
New England
ATTN: Chief, NEDED-T
ATTN: Library
North Atlantic
ATTN: Chief, NADEN-T
Middle East (Rear)
ATTN: MEDED-T
South Atlantic
ATTN: Chief, SADEN-TS
ATTN: Library
Huntsville
ATTN: Library (2)
ATTN: Chief, HNDED-CS
ATTN: Chief, HNDED-SR
Lower Mississippi Valley
ATTN: Library

[illegible] Engineer Div, [illegible]
[illegible]river
ATTN: Chief, Engr Div
ATTN: Library
North Central
ATTN: Library
Missouri River
ATTN: Library (2)
ATTN: Chief, MRDED-T
Southwestern
ATTN: Library
ATTN: Chief, SWDED-T
South Pacific
ATTN: Chief, SPDED-TG
Pacific Ocean
ATTN: Chief, Engr Div
North Pacific
ATTN: Chief, Engr

Facilities Engineers
FORSCOM
Ft Campbell, KY 42223
Ft Devens, MA 01[illegible]
Ft Carson, CO 80913
Ft Lewis, WA 98433
Ft Riley, KS 66442
Ft Polk, LA 71459
Ft Ord, CA 93941
USAECOM
Ft Monmouth, NJ 07703
USAIC (2)
Ft Benning, GA 31905
USAAVNC
Ft Rucker, AL 36361
CAC&FL
Ft Leavenworth, KS 66027
USACC
Ft Huachuca, AZ 85613
TRADOC
Ft Monroe, VA 23651
Ft Gordon, GA 30905
Ft Sill, OK 73503
Ft Bliss, TX 79916

AF/PREEU
Bolling AFB, DC 20332

Det 1 HQ ADTC/PRT
Tyndall AFB, FL 32403

Director
6570 AMRL/BBE
ATTN: Dr. H. Von Gierke
ATTN: Jerry Speakman
ATTN: LTC D. Johnson, BBA
Wright-Patterson AFB, OH 45433

Nav Undersea Center, Code 401
ATTN: Bob Gales
ATTN: Bob Young
San Diego, CA 92132

Naval Air Station
ATTN: Ray Glass/Code 661
Building M1
Naval Air Rework
North Island, CA 92135

US Naval Oceanographic Office
WASH DC 20373

Naval Air Systems Command
WASH DC 20360

NAVFAC
ATTN: Code 04
ATTN: David Kurtz/Code 2013C
Alexandria, VA 22332

Port Hueneme, CA 93043
ATTN: Library (Code L08A)

Washington, DC
ATTN: Building Research Advisory Board
ATTN: Transportation Research Board
ATTN: Library of Congress (2)
ATTN: Dept of Transportation Library

Aberdeen Proving Ground, MD 21005
Human Engineering Laboratory
ATTN: J. E. Weisz/AMZHE
ATTN: George Garinther
Ballistics Research Laboratory
ATTN: Bill Taylor
Army Environmental Hygiene Agency
ATTN: CPT George Luz/BioAcoustics

Defense Documentation Center (12)

Federal Aviation Administration
ATTN: M. B. Safeer, Chief
Envr Policy Div

National Bureau of Standards
ATTN: Dan R. Flynn

Bureau of National Affairs
ATTN: Fred Blosser, Rm 462

Office of Noise Abatement
ATTN: Gordon Banerian

Dept of Housing and Urban Development
ATTN: George Winzer, Chief Noise
Abatement Program

NASA
ATTN: H. Hubbard
ATTN: D. Hilton

EPA Noise Office
ATTN: Al Hicks, Rm 2113
ATTN: Dr. Kent Williams, Rm 109
ATTN: Tom O'Hara, Rm 907G

EPA Region III Noise Program
ATTN: Pat Anderson

Illinois EPA
ATTN: DMPC/Greg Zak
ATTN: Bob Hellweg

EPA
ATTN: AW-471/C. Caccavari
ATTN: AW-471/M. Nozick
ATTN: AW-371/A. Konheim
ATTN: R. Marrazzo
ATTN: W. Sperry
ATTN: J. Goldstein
ATTN: D. Gray
ATTN: D. Mudarri
ATTN: R. Hayman
ATTN: Robert A. Simmons

International Harvester
ATTN: Walter Page

Kamperman Associate, Inc.
ATTN: George Kamperman

Paul Borsky
Franklin Square, NY 11010

Booz-Allen Applied Research Div
ATTN: Robert L. Hershey, P.E.

Green Construction Co.
Charlie E. Sanders, VP

Cedar Knolls Acoustical Lab
ATTN: Dick Guernsey

USA Logistics Management Center
Bldg 12028
ATTN: MAJ R. Valentine

Federal Highway Administration
Region 15
ATTN: William Bowlby

Sensory Sciences Research Center
ATTN: Karl Kryter
ATTN: Jim Young

College of Law
ATTN: Mr. Plager

National Physical Laboratory (England)
Dr. Douglas W. Robinson

General Motors Proving Ground
ATTN: Ralph K. Hilliquis

Bolt Beranek and Newman, Inc.
ATTN: Ted Schultz
ATTN: Kenneth M. Eldred
ATTN: Dr. B. Galloway
ATTN: Dr. S. Fidell
ATTN: Dr. Pearsons

Engineering Societies Library
New York, NY 10017

Georgia Institute of Technology
ATTN: Clifford Bragdon

Dames and Moore
ATTN: Dr. F. M. Kessler

Pennsylvania State University
101 Engineering A Bldg
University Park, PA 16802

Westinghouse Electrical Corp
ATTN: Jim B. Moreland

Sandia Corporation
ATTN: Jack Reed

Society of Automotive Engrs
ATTN: William J. Toth

Wyle Labs
ATTN: L. Sutherland

Consolidated Edison Co., of NY
ATTN: Allan Teplitzky

Homans, Brian
Rotary wing aircraft operational noise data / B. Homans , L. Little , P. Schomer. -- Champaign, Ill. : Construction Engineering Research Laboratory ; Springfield, Va : for sale by National Technical Information Service, 1978.
iv. : ill. ; 27 cm. -- (Technical report - Construction Engineering Research Laboratory ; N-38)

1. Helicopters - noise. I. Little, Lincoln) II. Schomer, Paul D. III. U.S. Construction Engineering Research Laboratory. IV. Title. V. Series: U.S. Construction Engineering Research Laboratory. Technical report ; N-38.